NSWCDD/TR-93/429

PENETRATION OF SOLID AND LAYERED TARGETS BY GAS GUN-LAUNCHED STEEL CUBES

BY WILLIS MOCK, JR WILLIAM H. HOLT
WEAPONS SYSTEMS DEPARTMENT

JULY 1994

NAVAL SURFACE WARFARE CENTER
DAHLGREN DIVISION
Dahlgren, Virginia 22448-5100

NSWCDD/TR-93/429

PENETRATION OF SOLID AND LAYERED TARGETS BY GAS GUN-LAUNCHED STEEL CUBES

BY WILLIS MOCK, JR. WILLIAM H. HOLT
WEAPONS SYSTEMS DEPARTMENT

JULY 1994

NAVAL SURFACE WARFARE CENTER
DAHLGREN DIVISION
Dahlgren, Virginia 22448-5100

FOREWORD

Penetration mitigation techniques have been investigated for munition shielding applications. These techniques include the use of conventional monolithic materials as well as various combinations of layered materials to mitigate bullet and/or fragment impact hazards. The objectives of the work are twofold: (1) to conduct experiments on a variety of material specimens and evaluate their relative shock and penetration mitigating properties in a velocity range that yields performance differences (2000 - 3100 ft/sec for the material thicknesses studied), and (2) compare the results with respect to the types of target deformations and fractures.

Funding for this work was provided by the Navy Insensitive Munitions Advanced Development (IMAD) Program (Project Element 63609N).

The authors would like to acknowledge D. Crisp and M. Vittoria for providing the target materials that were developed by Battelle, and E. Rowe, Jr. for providing the Kevlar composite material. Also acknowledged are R. Lowry and J. Clark for helpful discussions concerning plate perforation damage and Dale Taylor for providing post-impact metallographic analysis for selected targets.

This report has been reviewed by T. E. Swierk, IMAD Ordnance Technology Coordinator, W. E. Hoye, Head, Warheads Branch, and D. L. Brunson, Head, Missile Systems Division.

Approved by:

David S. Malyevac

DAVID S. MALYEVAC, Deputy Head
Weapons Systems Department

ABSTRACT

A series of 14 impact experiments has been performed in which solid and layered targets nominally 3 x 3-in. by 0.5-in. thick have been impacted by 0.5-in. steel cubes in a flat-faced orientation. The number of target layers varied from one to five. The areal density of the targets ranged from 3.6 to 11.1 gm/cm^2. Three experiments were performed at an impact velocity ranging from 2000 to 2500 ft/sec and eleven experiments were performed at a velocity of approximately 3100 ft/sec. Target perforation did not occur in six of the higher velocity experiments. For these experiments, the number of target layers was either one or two. Target perforation occurred in five of the higher velocity experiments; the number of target layers was either three, four, or five for these experiments. Target failure consisted of one or more of the following types: cratering, shear bands, shear plugging, fracture, plate bending, petalling, and fiber breaking.

The impact resistance of a single flat-faced 1018 steel target was not significantly improved by machining a series of parallel ribs on the impact face of a target plate with the same areal density. These targets failed by a combination of shear banding and bending fracture. The results for the two-layer target of 1018 steel and Kevlar/epoxy composite showed that less steel fracture occurred when the composite was placed on the back surface of the impacted steel layer rather than on front of it. For the two-layer aluminum oxide-based cermet-304 stainless steel target, the brittle cermet layer fragmented on cube impact, but only plate bulging and bending occurred in the back surface steel layer.

Target perforation occurred in all of the three-, four-, and five-layer targets. The three-layer 1018 steel target had less impact resistance than the steel single-layer target with the same total thickness. In general, for the metal layered targets, the impacted layer failed by shear plugging and the back surface layer failed by plate bending, petalling, and fracture. Some permanent separation of the metal plates occurred for all the metal-layered-target experiments.

CONTENTS

	Page
I. INTRODUCTION	1
II. EXPERIMENTAL PROCEDURE	3
III. RESULTS	7
IV. SUMMARY AND CONCLUSIONS	20
REFERENCES	21
APPENDIXES	
A–PHOTOGRAPHS OF RECOVERED TARGET PLATES AND CUBES FOR EACH EXPERIMENT	A-1
DISTRIBUTION	(1)

ILLUSTRATIONS

Figure		Page
1	SCHEMATIC OF GAS GUN WITH SABOT STRIPPER	2
2	SCHEMATIC OF SABOT STRIPPER WITH ATTACHABLE SMALL TARGET ASSEMBLY	2
3	OVERVIEW OF GAS GUN FROM BREECH END	3
4	COMPLETED SABOT WITH CUBE, FRANGIBLE VACUUM COVER, AND STEEL TARGET PLATE	4
5	SECTIONED TARGET FOR EXPERIMENT 1	10

ILLUSTRATIONS (CONTINUED)

Figure		Page
6	SECTIONED TARGET FOR EXPERIMENT 2	10
7	SECTIONED TARGET FOR EXPERIMENT 3	11
8	SECTIONED TARGET FOR EXPERIMENT 4	11
9	SECTIONED TARGET FOR EXPERIMENT 5	12
10	SECTIONED TARGET FOR EXPERIMENT 6	12
11	SECTIONED TARGET FOR EXPERIMENT 7	13
12	SECTIONED TARGET FOR EXPERIMENT 8	13
13	SECTIONED TARGET FOR EXPERIMENT 9	14
14	SECTIONED TARGET FOR EXPERIMENT 10	14
15	SECTIONED TARGET FOR EXPERIMENT 11	15
16	SECTIONED TARGET FOR EXPERIMENT 12	15
17	SECTIONED TARGET FOR EXPERIMENT 13	16
18	SECTIONED TARGET FOR EXPERIMENT 14	16
19	1018 STEEL TARGET PLUG PIECE FOR EXPERIMENT 4	18

TABLES

Table		Page
1	DETAILED DESCRIPTIONS OF TARGETS	5
2	SUMMARY OF EXPERIMENTAL RESULTS	8

I. INTRODUCTION

This report describes the results of a series of impact experiments in which selected solid and layered targets were impacted with 0.5 in. cubes that were sabot-launched in a flat-faced orientation. The impact velocities ranged from 2000 to 3100 ft/sec. A sabot stripper was used to separate the sabot from the cube prior to impacting the target plate.[1]

Figure 1 is a schematic of the Naval Surface Warfare Center Dahlgren Division (NSWCDD) 40-mm smooth bore gas gun[2] that was used for the experiments. Figure 2 is a schematic of the sabot stripper. A target is secured between the mounting and clamp plates that attach to the stripper. The plates have concentric 2.234-in.-diameter holes. The target assembly is offset 2.25-in. from the back of the steel anvil. A sabot with an attached cube is loaded into the barrel, and a thin film mica vacuum cover is attached to the gun muzzle. The breech pressure vessel is filled with either helium or nitrogen gas to the desired pressure. The barrel is evacuated before firing the gas gun. The gun is fired by actuating the fast-opening valve, and the gas accelerates the sabot towards the gun muzzle. The sabot velocity is measured at the muzzle with three charged pins in the side of the barrel. The sabot velocity can be varied from 100 to 3200 ft/sec. After exiting the gas gun muzzle, the launched sabot is stopped on impact by a series of replaceable aluminum and steel rubber-faced plates, and the cube moves unhindered through a hole in the steel anvil to impact the target plate. Figure 3 is an overview of the gas gun from the breech end.

The experimental procedure is presented in Section II. Section III contains the results. The summary and conclusions are in Section IV. Appendix A contains photographs of recovered target plates and cubes for each experiment.

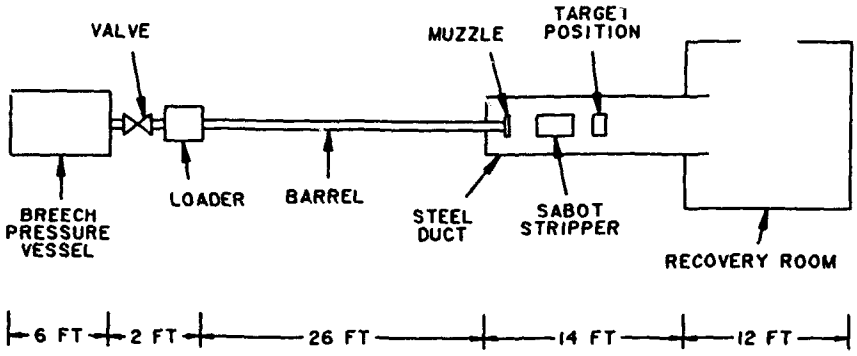

FIGURE 1. SCHEMATIC OF GAS GUN WITH SABOT STRIPPER

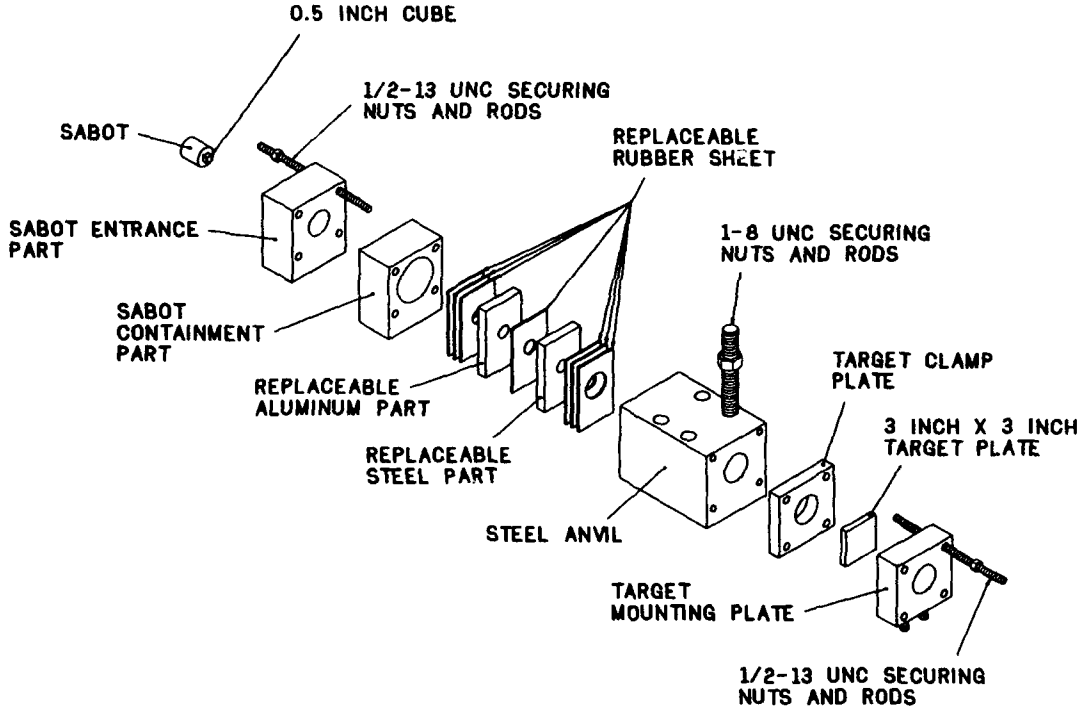

FIGURE 2. SCHEMATIC OF SABOT STRIPPER WITH ATTACHABLE SMALL TARGET ASSEMBLY

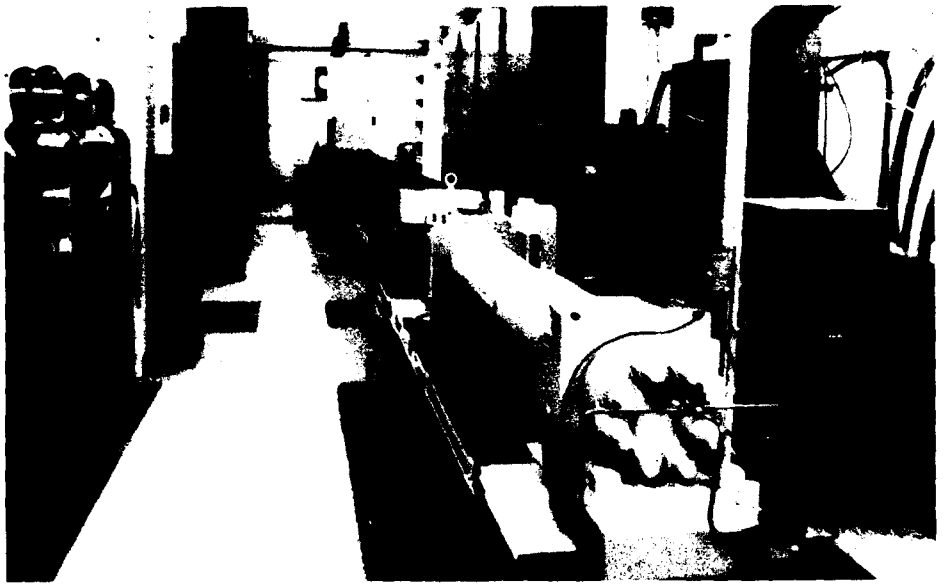

FIGURE 3. OVERVIEW OF GAS GUN FROM BREECH END

II. EXPERIMENTAL PROCEDURE

A completed sabot with cube, vacuum cover, and 3x3-in. steel target plate are shown in Figure 4. An empty sabot, with and without O-rings, weighs 86 and 84.4 gm, respectively. The sabot weight was reduced by machining round holes in the impact face. The sabot has an 0.508-in.-square socket that is 0.130-in. deep for the 0.5-in. cube. A central threaded hole (10-24 UNC) in the base of the socket is filled with fast-curing epoxy to secure the cube. The cube is centered in the socket by placing 0.004-in.-thick mica strips between the four side surfaces of the cube and the sides of the socket. The strips are removed after the epoxy has cured to provide a centered cube that only contacts the sabot at the base of the socket. This helps to ensure torque-free separation of the cube from the sabot. The 0.5-in. cubes were cut from 1018 steel square rod with an average as-received width of 0.499 in. The average machined cube length was 0.499 in. The cubes were mounted in the sabots so that the machined flat surface of a cube impacted the target. The average cube mass was 15.77 gm.

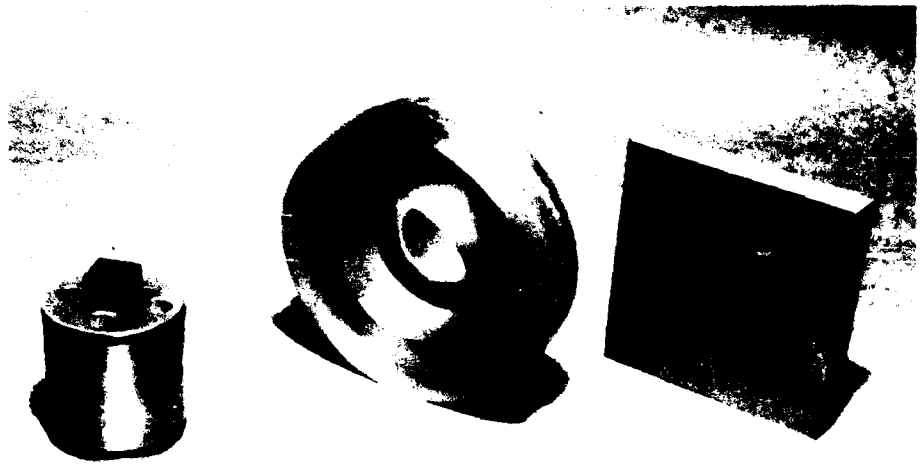

FIGURE 4. COMPLETED SABOT WITH CUBE, FRANGIBLE VACUUM COVER, AND STEEL TARGET PLATE

The vacuum cover permits evacuation of the gas gun barrel to prevent reduction of the sabot velocity by air pressure in the barrel. The vacuum cover is fabricated from a 1.8-in.-inside-diameter polycarbonate support ring and a frangible annulus of 0.004-in.-thick polyester film with a 1.000-in.-diameter center hole. The polyester annulus is covered by a disk of 0.001-in.-thick aluminum foil. The polyester film supports the aluminum foil against atmospheric pressure except in the center. The cube only impacts the 0.001-in.-thick aluminum foil as the cube and sabot exit the barrel.

Fourteen experiments were performed. Table 1 lists the material, thickness, mass and percent of total mass for each target layer. The nominal target width dimensions are 3 x 3-in. unless otherwise noted. The number of target layers varied from one to five. Where possible, an attempt was made to have target masses near that of a 1018 steel target with dimensions of 3 x 3-in. and 0.5-in.-thick (approximately 576 gm). Nine targets had a mass that varied from 568 to 599 gm. The four targets that contained an aluminum layer had a target mass that varied from 206 to 474 gm, and the target that contained ceramic tile had a calculated mass of 634 gm.

TABLE 1. DETAILED DESCRIPTIONS OF TARGETS

Experiment Number[a]	Number of Target Layers	Material, Thickness, Mass, and Percent of Total Mass for Each Target Layer[b]				
		Layer 1	Layer 2	Layer 3	Layer 4	Layer 5
1	1	6061-T6 aluminum, 0.516 in., 206 gm, 100 %				
2	1	Mild Steel, 0.518 in., 599 gm, 100%				
3	1	1018 steel, 0.495 in., 569 gm, 100%				
4	1	1018 steel, 0.495 in., 570 gm, 100%				
5	1	1018 steel, narrow ribbed, 0.522 in., 569 gm, 100%				
6	1	1018 steel, wide ribbed, 0.545 in., 568 gm, 100%				
7	2	1018 steel, 0.416 in., 480 gm, 83%	Kevlar/epoxy composite, 0.507 in., 99 gm, 17%,			
8	2	Kevlar[c]/epoxy composite, 0.507 in., 99 gm, 17%	1018 steel, 0.417 in., 479 gm, 83%			
9	2	Aluminum oxide-based cermet, 0.366 in., 211 gm, 36%	304 stainless steel, 0.360 in., 376 gm, 64%			
10	3	1018 steel, 0.167 in., 192 gm, 34%	1018 steel, 0.166 in., 192 gm, 33%	1018 steel, 0.167 in., 192 gm, 33%		
11	3	Mild steel, 0.168 in., 182 gm, 43%	6061-0 aluminum, 0.172 in., 65 gm, 15%	Mild steel, 0.161 in., 175 gm, 42%		
12	4	Ceramic tile[d], 0.250 in., 70 gm, 11%	Torr-Seal epoxy[e], 0.039 in., 11 gm, 2%	Ceramic tile, 0.250 in., 70 gm, 11%	1018 steel, 0.380 in., 483 gm, 76%	
13	5	Mild steel, 0.175 in., 185 gm, 44%	Grade A titanium, 0.045 in., 27 gm, 6%	6061-0 aluminum, 0.086 in., 32 gm, 8%	Grade A titanium, 0.050 in., 31 gm, 7%	Mild steel, 0.143 in., 151 gm, 35%
14	5	Hadfield steel, 0.153 in., 179 gm, 38%	Grade A titanium, 0.051 in., 35 gm, 7%	6061-0 aluminum, 0.087 in., 36 gm, 8%	Grade A titanium, 0.051 in., 35 gm, 7%	Hadfield steel, 0.161 in., 189 gm, 40%

[a] The target layers are listed in the order in which they are impacted.

[b] Experiments 1 through 14 correspond to gas gun shots 459, 460, 468, 469, 489, 492, 494, 495, 490, 501, 491, 493, 470, and 471, respectively. The targets for experiments 9, 11, 13, and 14 were provided by Battelle.[3]

[c] Trademark of aromatic polyamide fiber manufactured by E. I. duPont de Nemours & Co., Wilmington, DE 19898.

[d] U275 Wall Tile, Part No. 22352, United States Ceramic Tile Co., East Sparta, OH 22352

[e] Varian Associates, Palo Alto, CA.

The narrow-ribbed steel target plate for Experiment 5 contains 16 parallel ribs. The semi-circular cross-section ribs are 0.125 in. wide and 0.0625 in. high with a 0.0625 in. space between them. This gives a solid target thickness of 0.460 in. out of a total target thickness of 0.522 in. The wide-ribbed steel target plate for Experiment 6 contains nine ribs. The semi-circular cross-section ribs are 0.250 in. wide and 0.125 in. high with an 0.09375 in. space between them. This gives a solid target thickness of 0.420 in. out of a total target thickness of 0.545 in. Hardman fast-setting epoxy (several thousandths inch thick layer) was used to bond the steel and ceramic tile materials together for Experiments 7 and 8. The three steel layers for Experiment 11 were clamped together and not bonded with epoxy.

The completed targets for Experiments 9, 11, 13, and 14 were provided by Battelle.[3] The Battelle identification numbers are C5-4PM, 1174-3 x 3-2, 1173-3 x 3-3, and 1179-3 x 3-1 for the nominally 3 x 3-in. flat target plates for Experiments 9, 11, 13, and 14, respectively. The metal target layers for Experiments 11, 13, and 14 were explosively bonded. The two-layer cermet-metal target plate for Experiment 9 was fabricated by depositing a cermet of aluminum oxide (Al_2O_3) onto a nominally 3 x 3 x 3/8-in.-thick 304 stainless steel substrate and then cold and hot pressing the specimen using powder metallurgy techniques. The resulting compressed cermet coating density was about 75 percent of the theoretical maximum density.[3]

The masses of the individual target layers for Experiments 9, 11, 13, and 14 were calculated since the layers had been bonded together into single units by Battelle. The following density values were used for these calculations: density of steel = 7.79 gm/cm^3 (average value for 1018 steel cubes for 14 experiments), density of titanium[4] = 4.50 gm/cm^3, density of aluminum = 2.71 gm/cm^3 (value calculated for 6061-T6 aluminum target plate from Experiment 1). A traveling microscope was used to measure the thickness of the layers for Experiments 11, 13, and 14 after impact. The cermet thickness and mass values for Experiment 9 were calculated using the steel values and the values for the two-layer target prior to impact. The ceramic tile for Experiment 12 was impacted without modifying the as-received size of 4.25 x 4.25-in. wide and 0.25-in. thick. The 70 gm mass for this material in Table 1 was calculated using the standard target width dimensions of 3 x 3 in.

III. RESULTS

Table 2 summarizes the experimental results. The target thicknesses varied from 0.495 to 0.919 in. and the target masses varied from 206 to 634 gm. The areal density increased from 3.55 gm/cm^2 for the 6061-T6 aluminum target in Experiment 1 to 11.12 gm/cm^2 for the aluminum cermet-steel layered target for Experiment 9. The cube impact velocity range was from 2010 to 3114 ft/sec. The selected velocity was 2010 and 2013 ft/sec for two shots, 2516 ft/sec for a single shot, and varied between 3037 and 3114 ft/sec for 11 shots. The estimated target damage and target perforation descriptions are also given for each experiment. Appendix A contains photographs of the recovered target plates and cubes for each experiment. Figures 5 through 18 are photographs of the recovered targets after they were sectioned through the impact region.

Figure 5 shows the result for a single 6061-T6 aluminum layer impacted at 2010 ft/sec in Experiment 1. An approximate 0.67-in. wide square plug was sheared from the target plate by the impacting cube.[5] The recovered cube width decreased from approximately 0.67 in. at the impact end to 0.5 in. at the free surface end; the cube length decreased by approximately 9 percent in the center to approximately 20 percent at the cube edges.

The effect of increasing cube velocity on target damage for a single mild steel target layer is given in Figures 6 through 8. Target cratering was observed for the 2013 and 2516 ft/sec impact velocity experiments. For the 3106 ft/sec higher velocity experiment, more extensive damage consisting of shear plug formation and fracture was observed. The crater diameter in the target impact plane was approximately 0.79 in. for all three experiments. The maximum crater depth was approximately 0.17, 0.28, and 0.82 in. for Experiments 2, 3, and 4, respectively. For Experiment 4, the deformed cube remained embedded in the crater; the crater depth for this experiment was measured to the bottom of the cube. (The crater depth was measured from the target impact plane.) Maximum cube width and length values of 0.83 in. and 0.37 in., respectively, were measured for the recovered cubes for Experiments 2 and 3.

TABLE 2. SUMMARY OF EXPERIMENTAL RESULTS

Experiment Number[a]	Number of Target Layers	Target Layer Materials[b]	Initial Thickness of Target (in.)	Initial Mass of Target (gm)	Average Target Density (gm/cm^3)
1	1	6061-T6 Aluminum	0.516	206	2.71
2	1	Mild steel	0.518	599	7.84
3	1	1018 steel	0.495	569	7.81
4	1	1018 steel	0.495	570	7.81
5	1	1018 steel, narrow ribbed	0.522	569	7.39
6	1	1018 steel, wide ribbed	0.545	568	7.09
7	2	1018 steel Kevlar/epoxy composite	0.923	579	4.31
8	2	Kevlar/epoxy composite 1018 steel	0.923	579	4.24
9	2	Aluminum oxide-based cermet 304 stainless steel	0.726	587	6.03
10	3	1018 steel 1018 steel 1018 steel	0.500	576	7.80
11	3	Mild steel 6061-0 aluminum Mild steel	0.501	422	6.04
12	4	Ceramic tile Torr-Seal epoxy Ceramic tile 1018 steel	0.919	634[d]	4.67
13	5	Mild steel Grade A titanium 6061-0 aluminum Grade A titanium Mild steel	0.499	423	6.27
14	5	Hadfield steel Grade A titanium 6061-0 aluminum Grade A titanium Hadfield steel	0.503	474	6.27

[a] The targets for Experiments 9, 11, 13, and 14 were provided by Battelle.[3]

[b] The target layers are listed in the order in which they were impacted.

[c] Obtained by multiplying the average target density by the target thickness.

[d] Calculated value using the 3 x 3-in. standard target width for the ceramic tile.

TABLE 2. SUMMARY OF EXPERIMENTAL RESULTS (CONTINUED)

Experiment Number[a]	Areal Density[c] (gm/cm^2)	Impact Velociity (ft/sec)	Target Perforated	Type of Target Damage
1	3.55	2010	Yes	Shear plugging
2	10.30	2013	No	Cratering with ductile deformation and plate bulging
3	9.81	2516	No	Cratering with ductile deformation and plate bulging
4	9.81	3106	No	Shear plugging and fracture
5	9.80	3101	No	Shear plugging and fracture
6	9.81	3064	No	Shear plugging and fracture
7	10.10	3084	No	Layer 1—Ductile bulging and fracture. Layer 2—Bending and breaking of fibers
8	9.95	3082	No	Layer 1—Catastrophic bending and breaking of fibers Layer 2—Bulging, fracture, and radial cracking
9	11.12	3037	No	Layer 1—Fracture Layer 2—Bulging and bending of plate
10	9.91	3091	Yes	Layer 1—Shear plugging Layer 2—Shear plugging, fracture, and plate bending Layer 3—Fracture, plate bending, and petaling
11	7.68	3079	Yes	Layer 1—Shear plugging Layer 2—Shear plugging Layer 3—Shear plugging, plate bending, petaling, and fracture
12	10.90	3070	Yes	Ceramic tile layers—Brittle fracture Steel layer—Plate bending and fracture
13	7.95	3112	Yes	Layers 1, 2, 3—Ductile hole formation and fracture Layer 4—Plate bending and shear fracture Layer 5—Plate bending and fracture
14	8.00	3114	Yes	Layer 1—Shear plugging Layers 2, 3, 4—Plate bending, shear, and fracture Layer 5—Plate bending, petaling, and fracture

FIGURE 5. SECTIONED TARGET FOR EXPERIMENT 1—0.516 IN.-THICK 6061-T6 ALUMINUM TARGET, SHEAR PLUG, AND IMPACT CUBE (SHOWN AT TOP), 2010 FT/SEC IMPACT VELOCITY, 206 GM TARGET MASS

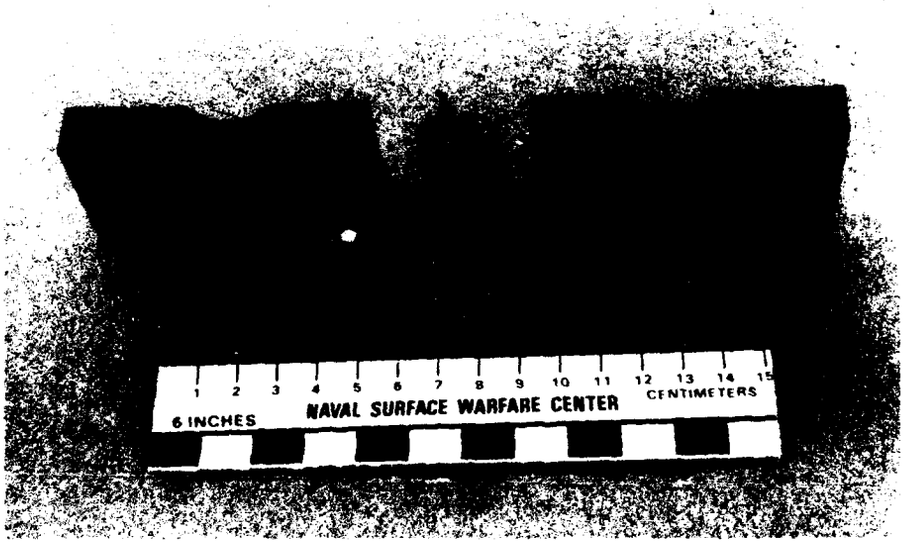

FIGURE 6. SECTIONED TARGET FOR EXPERIMENT 2—0.518-IN.-THICK MILD STEEL TARGET AND IMPACT CUBE, 2013 FT/SEC IMPACT VELOCITY, 599 GM TARGET MASS

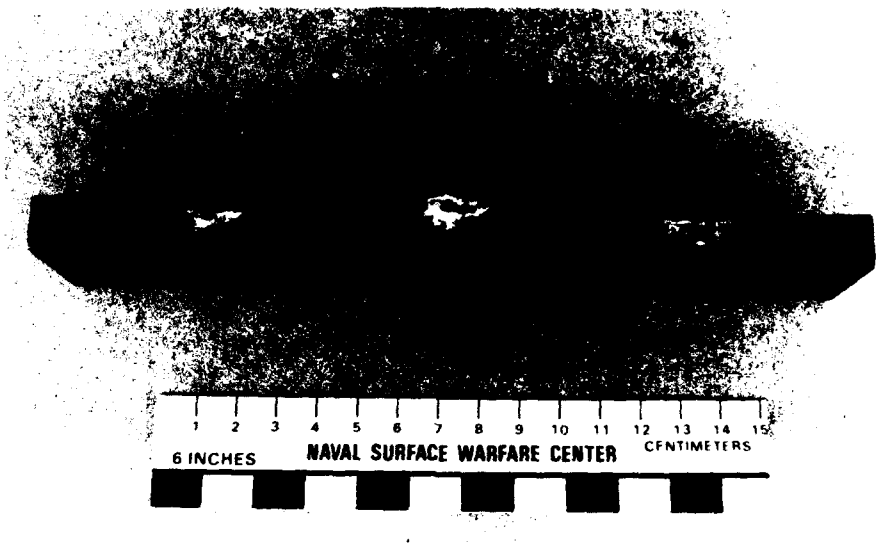

FIGURE 7. SECTIONED TARGET FOR EXPERIMENT 3—0.495-IN.-THICK 1018 STEEL TARGET PLATE AND IMPACT CUBE, 2516 FT/SEC IMPACT VELOCITY, 569 GM INITIAL TARGET MASS

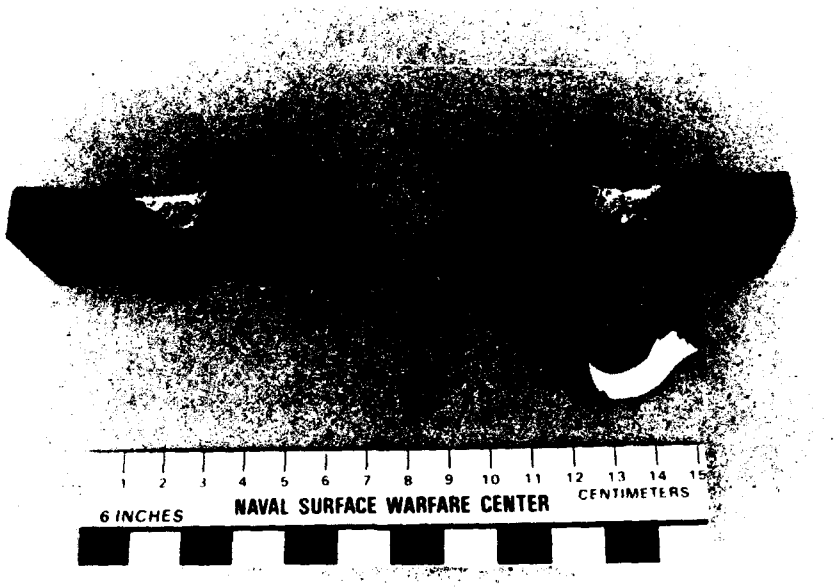

FIGURE 8. SECTIONED TARGET FOR EXPERIMENT 4—0.495-IN.-THICK 1018 STEEL TARGET AND EMBEDDED IMPACT CUBE, 3106 FT/SEC IMPACT VELOCITY, 570 GM TARGET MASS

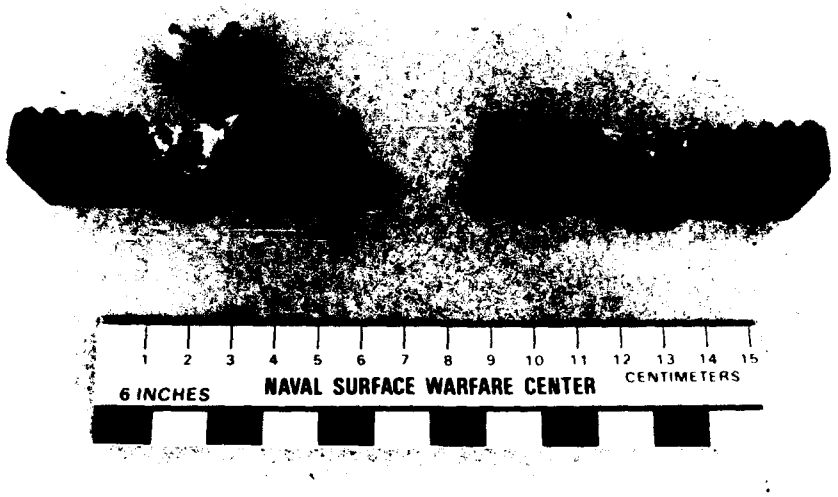

FIGURE 9. SECTIONED TARGET FOR EXPERIMENT 5—0.522-IN. -THICK NARROW-RIBBED 1018 STEEL TARGET AND EMBEDDED IMPACT CUBE, 3101 FT/SEC IMPACT VELOCITY, 569 GM TARGET MASS

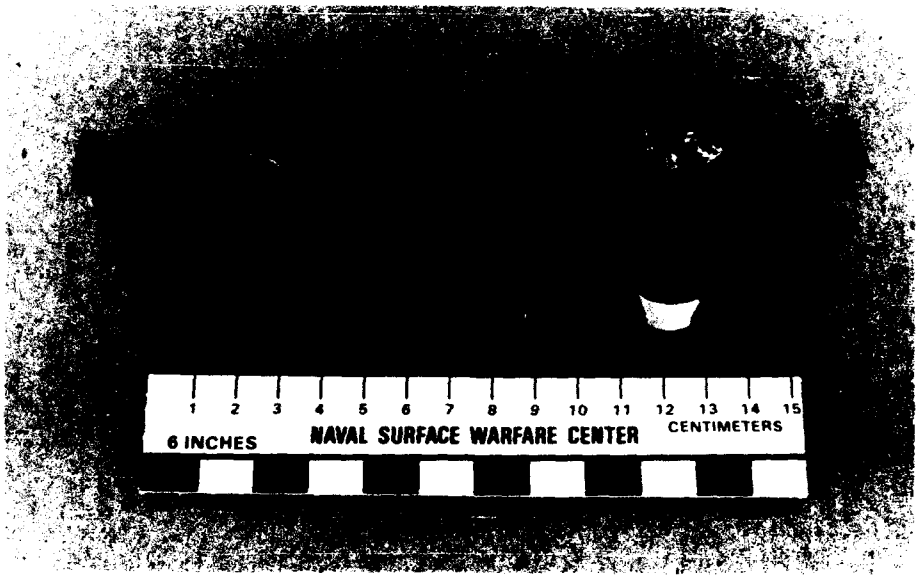

FIGURE 10. SECTIONED TARGET FOR EXPERIMENT 6—0.545-IN. -THICK WIDE-RIBBED 1018 STEEL TARGET AND EMBEDDED IMPACT CUBE, 3064 FT/SEC IMPACT VELOCITY, 568 GM TARGET MASS

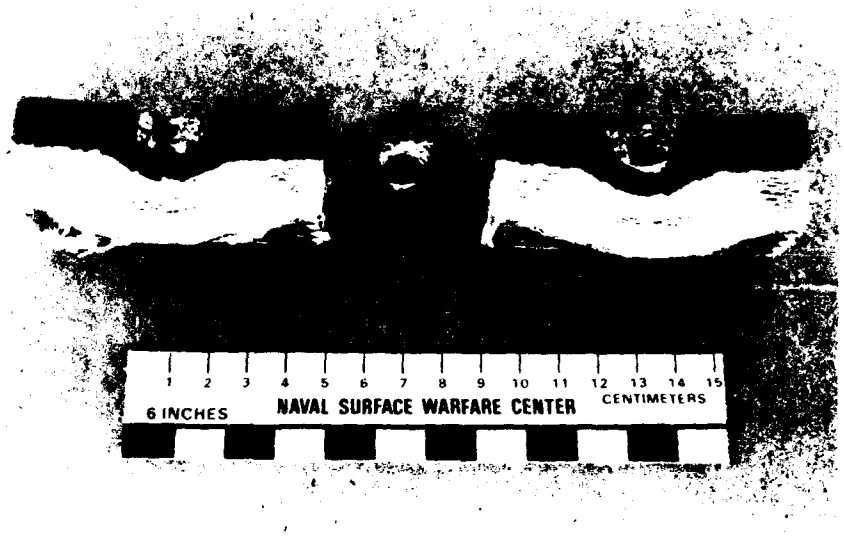

FIGURE 11. SECTIONED TARGET FOR EXPERIMENT 7—0.923-IN.-THICK TWO-LAYER 1018 STEEL-KEVLAR/EPOXY TARGET AND IMPACT CUBE, 3084 FT/SEC IMPACT VELOCITY, 579 GM TARGET MASS

FIGURE 12. SECTIONED TARGET FOR EXPERIMENT 8—0.923-IN.-THICK TWO-LAYER KEVLAR/EPOXY-1018 STEEL TARGET AND EMBEDDED IMPACT CUBE, 3082 FT/SEC IMPACT VELOCITY, 579 GM TARGET MASS

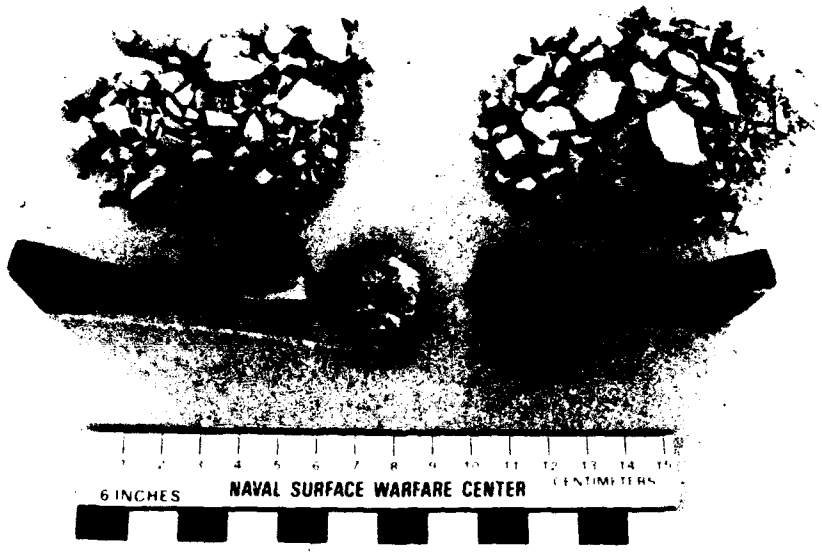

FIGURE 13. SECTIONED TARGET FOR EXPERIMENT 9—0.726-IN.-THICK TWO-LAYER ALUMINUM OXIDE-BASED CERMET-304 STAINLESS STEEL TARGET AND IMPACT CUBE, 3037 FT/SEC IMPACT VELOCITY, 587 GM TARGET MASS

FIGURE 14. SECTIONED TARGET FOR EXPERIMENT 10—0.500-IN.-THICK THREE-LAYER 1018 STEEL TARGET, FRAGMENT PIECES, AND IMPACT CUBE (SHOWN IN MIDDLE), 3091 FT/SEC IMPACT VELOCITY, 576 GM TARGET MASS

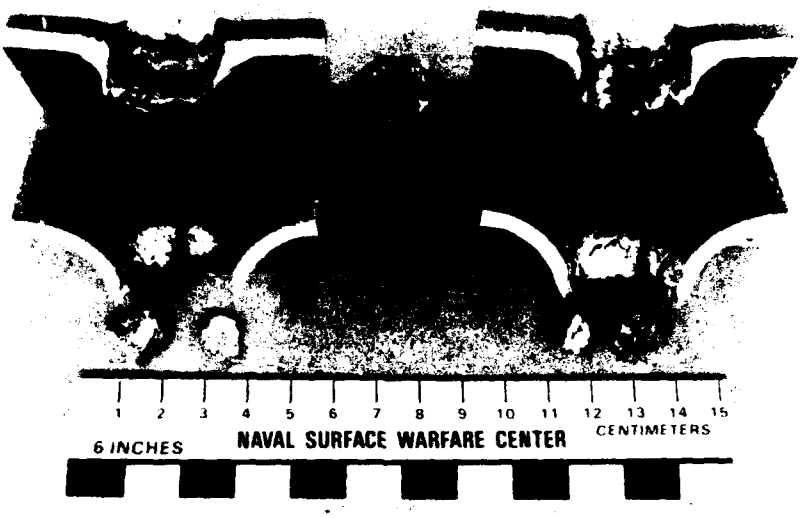

FIGURE 15. SECTIONED TARGET FOR EXPERIMENT 11—0.501-IN.-THICK THREE-LAYER MILD STEEL-6061-0-ALUMINUM-MILD STEEL TARGET, FRAGMENT PIECES, AND IMPACT CUBE (SHOWN IN MIDDLE), 3079 FT/SEC IMPACT VELOCITY, 422 GM TARGET MASS

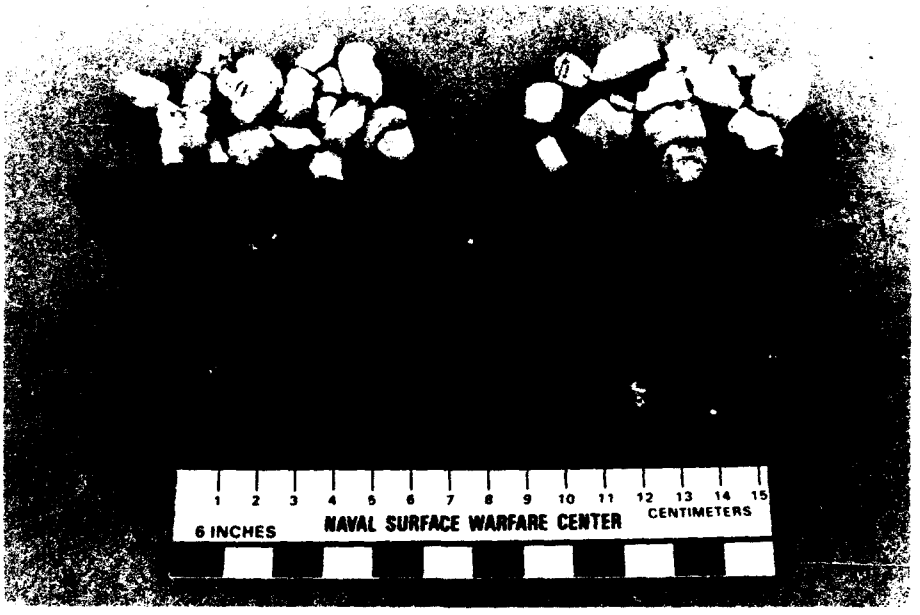

FIGURE 16. SECTIONED TARGET FOR EXPERIMENT 12—0.919-IN.-THICK FOUR-LAYER CERAMIC TILE-TORR-SEAL EPOXY-CERAMIC TILE-1018 STEEL TARGET, FRAGMENT PIECES, AND IMPACT CUBE (SHOWN IN MIDDLE), 3070 FT/SEC IMPACT VELOCITY, 634 GM TARGET MASS

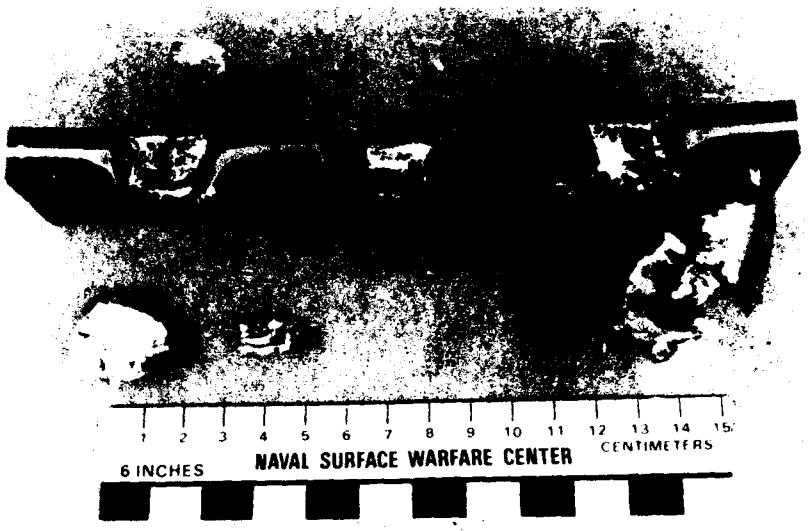

FIGURE 17. SECTIONED TARGET FOR EXPERIMENT 13—0.499-IN.-THICK FIVE-LAYER MILD STEEL-GRADE A TITANIUM-6061-0 ALUMINUM-GRADE A TITANIUM-MILD STEEL TARGET, FRAGMENT PIECES, AND IMPACT CUBE (SHOWN IN CENTER), 3112 FT/SEC IMPACT VELOCITY, 423 GM TARGET MASS

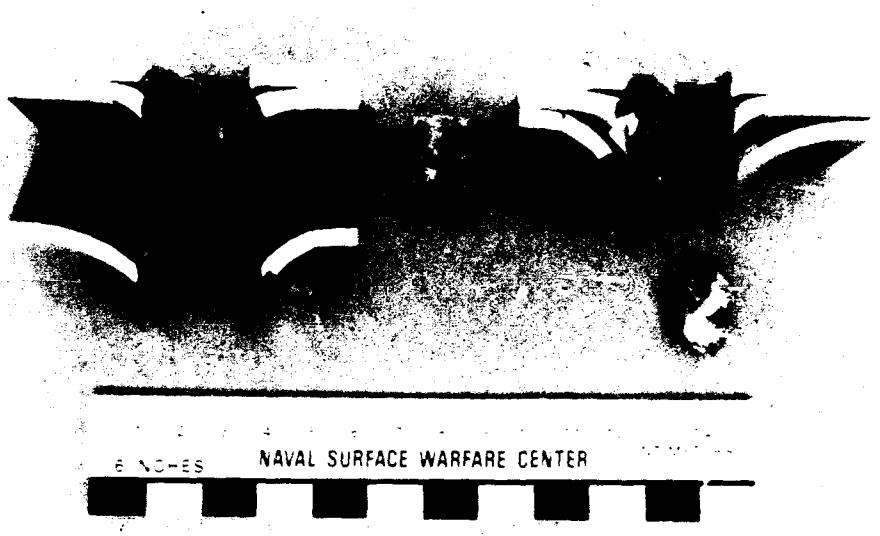

FIGURE 18. SECTIONED TARGET FOR EXPERIMENT 14—0.503-IN.-THICK FIVE-LAYER HADFIELD STEEL-GRADE A TITANIUM-6061-0 ALUMINUM-GRADE A TITANIUM-HADFIELD STEEL TARGET, FRAGMENT PIECES AND IMPACT CUBE (SHOWN IN CENTER), 3114 FT/SEC IMPACT VELOCITY, 474 GM TARGET MASS

Figure 19 shows two types of fractures that were observed on the ejected plug piece for the 3106 ft/sec impact experiment. This mixed failure mode (shear bands and bending fracture) can also be observed in the nonejected plug piece in Figure 8 and has been described by Woodward.[6,7] In this description, when plugging is initiated by shear bands on one side of the plug, asymmetries can develop when the bands reach the rear surface of the target causing slip to more easily occur. The plug can then bend and tear in nonshear surface regions.

No target perforation occurred for Experiments 2, 3, and 4, although for the 3106 ft/sec impact experiment, the back surface plug bulge was approximately 0.5 in. (the plate thickness). The extensive target damage suggests that 3106 ft/sec is probably near the perforation threshold for this target.

Figures 9 and 10 show the effect of adding a series of narrow and wide ribs, respectively, to the impact face of the 1018 steel target plates. This approach is a variation on a spall mitigation technique.[8] The target mass and areal density for these experiments was the same as for the flat single layer 1018 steel target plates for Experiments 3 and 4. The same mixed failure mode consisting of shear bands and bending fracture that was observed for Experiment 4 was also observed for Experiments 5 and 6. No target perforation occurred. The deformed cube remained embedded in the crater for Experiments 5 and 6. Incomplete shear plugs had begun to form for both experiments. Back surface plug bulge of approximately 0.4 and 0.6 in., respectively, was observed for the narrow- and wide-ribbed steel targets. Also, asymmetries were introduced by the ribs since for both experiments the side of the plug that showed incomplete shear or fracture damage was a side that was perpendicular to the direction of the ribs on the impact surface (see Figures A-5 and A-6).

Figures 11 and 12 show the results of a cube impact with a two-layer steel-Kevlar/epoxy target and a two-layer Kevlar/epoxy-steel target, respectively. These figures show that less target damage occurred by placing the Kevlar/epoxy composite layer behind the steel layer than in front of it. Fracture and a noticeable back surface bulge occurred in the steel target layer for Experiment 7. A bulge of approximately 0.32 in. was measured for the 0.416-in.-thick steel layer. The Kevlar/epoxy composite layer had a back surface bulge of approximately 0.37 in. Some composite delamination and broken Kelvar fibers occurred near the back surface of the composite.

(a)

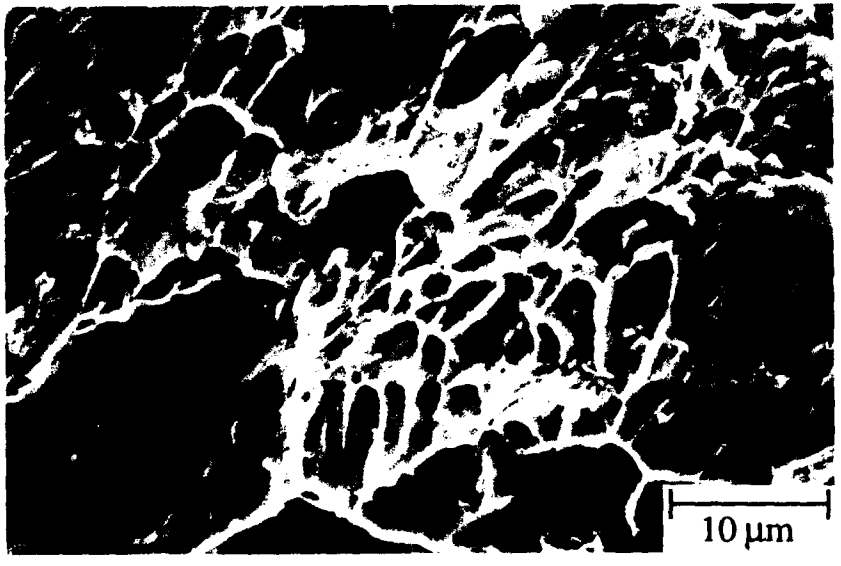

(b)

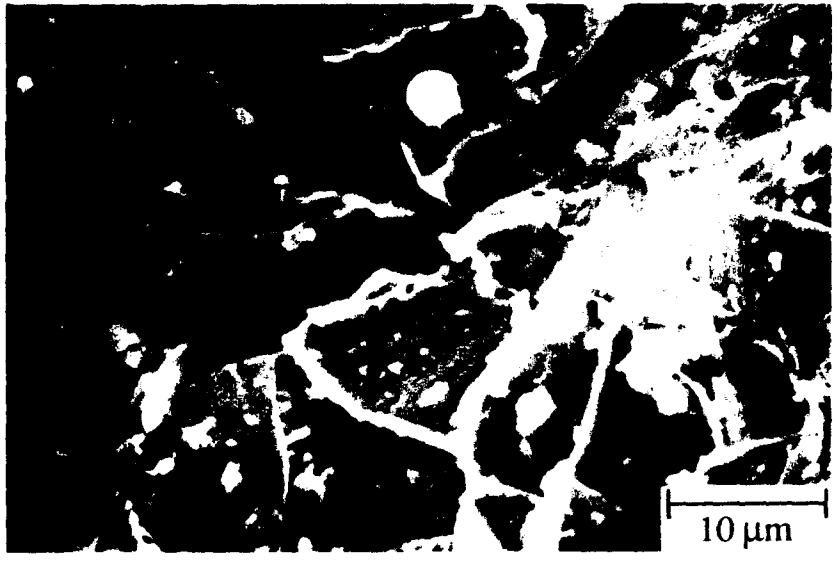

(c)

FIGURE 19. 1018 STEEL TARGET PLUG PIECE FOR EXPERIMENT 4 SHOWNING (A) PLUG PIECE AND SEM MICROGRAPHS OF (B) SHEAR DIMPLE AND (C) CLEAVAGE FRACTURE REGIONS

Damage was more extensive for the target in Experiment 8. The Kevlar/epoxy composite layer suffered catastrophic damage by the impacting steel cube. The steel layer for this experiment failed mainly by plate bending and fracture. A shear fracture surface of limited extent was observed adjacent to the back surface of the steel plate. The target mass and impact velocity for Experiments 7 and 8 is the same as that for Experiment 4.

Figure 13 shows the result for the two-layer aluminum oxide-based cermet-304 stainless steel target impacted in Experiment 9. The cermet layer fractured into many pieces. Plate bending was observed for the steel layer; no cracks were observed in the steel plate. A back surface bulge of approximately 0.4 in. was measured for the 0.360-in.-thick steel plate. For this experiment, the post-impact cube height was approximately 0.25 in., which corresponds to a 50 percent reduction in this dimension.

The target for Experiment 10 is a 0.500-in.-thick three layer 1018 steel target. Each target layer is the same thickness. This experiment was performed to compare with the result for Experiment 4 (a single 0.495-in.-thick 1018 steel layer). The Experiment 10 result is shown in Figure 14. Complete target perforation occurred. Plate 1 failed mainly by shear plug formation; only a minimum amount of plate bending occurred and no radial tearing was observed. Plate 2 failed by a combination of shear plug formation, plate bending and some radial tearing. Plate 3 failed by plate bending, petaling, and fracture. The recovered mushroomed cube for this experiment had a small approximately 0.020-in.-deep by 0.070-in. wide hole in the center of the impact face.

The result for the explosively bonded three-layer mild steel-6061-0 aluminum-mild steel target is shown in Figure 15. Layers 1 and 2 failed primarily by shear banding with no radial tearing and minimum plate bending occurring. Layers 1 and 2 did not separate from each other although in the sectioned target some large interface cracks were evident adjacent to the cube impact area. Layer 3 separated during impact (Figure 15). It failed by shear banding, plate bending, petaling, and fracture. Complete perforation occurred for this target. The recovered cube for this shot also had a hole in the center of the impact face (approximately 0.150-in. diameter by 0.070-in. deep) and several cracks on the back face. The cracks were in a cross pattern that extended partway across the cube face and towards the cube edges.

The result for the multi-layer target for Experiment 12 is shown in Figure 16. Target perforation occurred for this experiment. The ceramic tile layers fragmented into many pieces. Only the larger fragments are shown in Figure 16. The steel layer failed mainly by plate bending, and radial and circumferential cracking. The layer fragmented into five large pieces. A ring fracture pattern was observed on the back surface of the two larger plate pieces.[9] A shear lip fracture was observed on the back of several of the smaller fragment pieces.

The result for the explosively bonded five-layer mild steel-titanium-aluminum-titanium-mild steel target is shown in Figure 17. Target perforation occurred for this experiment. Minimum fracture and delamination occurred for the first three layers. Figure 17 shows that material for these three layers was pushed ahead of the impacting cube and then aside since steel layer material flowed approximately 0.6 in. beyond the impact face. Layers 4 and 5 were delaminated, bent, and almost torn from the target by the impacting cube. The titanium layer 4 failed mainly in shear. The back surface steel layer failed by plate bending and fracture.

Figure 18 shows the result for the explosively bonded five-layer Hadfield steel-titanium-aluminum-titanium-Hadfield steel target for Experiment 14. Target delamination consisted primarily of separation of the steel layers from the target. The initial steel layer failed primarily by shear plug formation. Figure 18 suggests that layers 2, 3, and 4 failed by a combination of plate bending, shear, and fracture. The back surface steel layer failed by plate bending, petaling, and fracture.

IV. SUMMARY AND CONCLUSIONS

A series of fourteen impact experiments has been performed in which solid and layered targets nominally 3 x 3-in. by 0.5-in. thick have been impacted by 0.5-in. cubes in a flat-faced orientation. The number of target layers varied from one to five. The areal density of the targets ranged from 3.6 to 11.1 gm/cm^2. Three experiments were performed at an impact velocity ranging from 2000 to 2500 ft/sec and eleven experiments were performed at a velocity of approximately 3100 ft/sec. Target perforation did not occur in six of the higher velocity experiments. For these experiments the number of target layers was either one or two. Target perforation

occurred in five of the higher velocity experiments; the number of target layers was either three, four, or five for these experiments. Target failure consisted of one or more of the following types: cratering, shear bands, shear plugging, fracture, plate bending, petaling, and fiber breaking.

The impact resistance of a single flat-faced 1018 steel target (Experiment 4) was not significantly improved by machining a series of parallel ribs on the target impact face while maintaining the same areal density (Experiments 5 and 6). These targets failed by a combination of shear banding and bending fracture. The results for the two-layer target of 1018 steel and Kevlar/epoxy composite showed that less steel fracture occurred when the composite was placed on the back surface of the impacted steel layer (Experiment 7) rather than on front of it (Experiment 8). For the two-layer aluminum oxide-based cermet-304 stainless steel target (Experiment 9), the brittle cermet layer fragmented on cube impact but only plate bulging and bending occurred in the back surface steel layer.

Target perforation occurred in all of the three-, four-, and five-layer targets. The three-layer 1018 steel target (Experiment 10) had less impact resistance than the steel single-layer target with the same total thickness (Experiment 4). In general, for the metal layered targets, the impacted layer failed by shear plugging and the back surface layer failed by plate bending, petaling, and fracture. Some permanent separation of the metal plates occurred for all the metal-layered-target experiments.

REFERENCES

1. Mock, Jr., Willis and Holt, W. H., *Nonaerodynamic Sabot Stripper for NSWCDD 40-mm Gas Gun*, NSWCDD/TR-92/447, Naval Surface Warfare Center, Dahlgren Division, Dahlgren, VA 22448-5000, November 1992.

2. Mock, Jr., Willis and Holt, W. H., *The NSWC Gas Gun Facility for Shock Effects in Materials*, NSWC/DL TR-3473, Naval Surface Weapons Center, Dahlgren Laboratory, Dahlgren, VA 22448-5000, July 1976.

3. Foster, Jr., E. L; Peterson, J.; and Onesto, E., *Development/Evaluation of Penetration Resistant Materials/Structural Concepts*, Special Task 0001CR, Contract DLA900-83-C-1744, Battelle, Columbus, OH, to Naval Surface Warfare Center, Dahlgren, VA, November 1990.

4. Michaels, T. E.; Isbell, W. M.; and Babcock, S. G., *Measurements of Dynamic Properties of Materials, Vol. IV, Alpha Titanium*, DASA 2501-4, Materials and Structures Laboratory, General Motors Corporation, General Motors Technical Center, Warren, MI, February 1972.

5. Woodward, R. L.; Baxter, B. J.; and Scarlett, N. V. Y., "Mechanisms of Adiabatic Shear Plugging Failure in High Strength Aluminum and Titanium Alloys," in *Mechanical Properties of High Rates of Strain*, Harding, J., Ed., published by Institute of Physics, London England, 1984, pp. 525-532.

6. Woodward, R. L., "Material Failure at High Strain Rates," in *High Velocity Impact Dynamics*, Zukas, Jonas A., John Wiley and Sons, Inc., New York, N. Y., 1990, pp. 65-125.

7. Woodward, R. L., "The Interrelation of Failure Modes Observed in the Penetration of Metallic Targets," *International Journal of Impact Engineering*, Vol. 2, 1984, pp. 121-129.

8. Smith, J. H., "Three Low-Pressure Spall Thresholds in Copper," in *Symposium on Dynamic Behavior of Materials, ASTM Materials Science Series-5*, published by American Society for Testing of Materials, Philadelphia, PA, 1963, pp. 264-281.

9. Goldsmith, W. and Finnegan, S. A., "Normal and Oblique Impact of Cylindo-Conical and Cylindrical Projectiles on Metallic Plates," *International Journal of Impact Engineering*, Vol. 4, 1986, pp. 83-105.

APPENDIX A

PHOTOGRAPHS OF RECOVERED TARGET PLATES AND CUBES FOR EACH EXPERIMENT

This appendix contains photographs of the recovered target plates and either embedded or separate impact cubes for each experiment. Figures A-1(a) through A-14(a) show the impact surface of the target plates and Figures A-1(b) through A-14(b) show the back surface of the target plates. Some figures (Figures A-5(c) through A-14(c) show a side view of the plates. Cube motion was from left to right in Figures A-5(c) through A-12(c) and right to left in Figures A-13(c) and A-14(c). The figures also show some fragment pieces for fragmented ceramic targets or perforated metal targets. For some experiments, the inner surface of the layered targets is also shown.

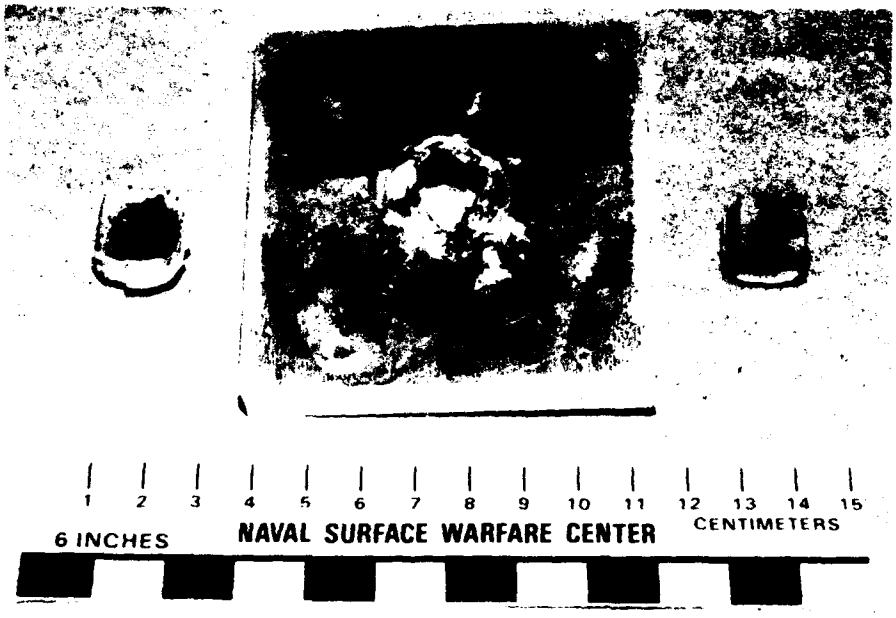

(a) Impact Surface of Aluminum Plate and Sheared Plug; Back Surface of Cube (Shown on Right)

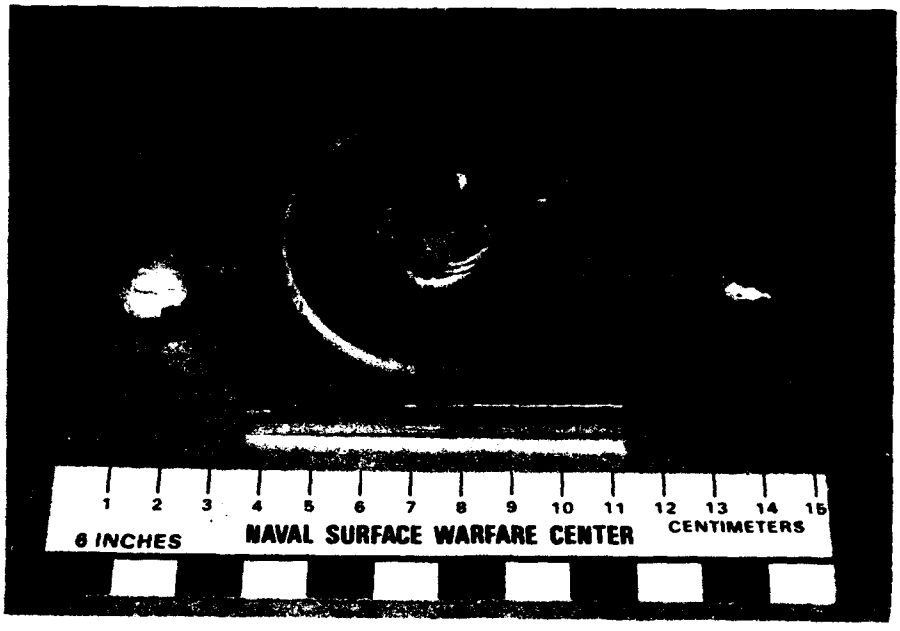

(b) Back Surface of Aluminum Plate and Sheared Plug; Impact Surface of Cube (Shown on Right)

FIGURE A-1. RECOVERED 0.516-IN.-THICK 6061-T6 ALUMINUM TARGET PLATE AND CUBE FOR EXPERIMENT 1 (TARGET MASS = 206 GM; IMPACT VELOCITY = 2010 FT/SEC)

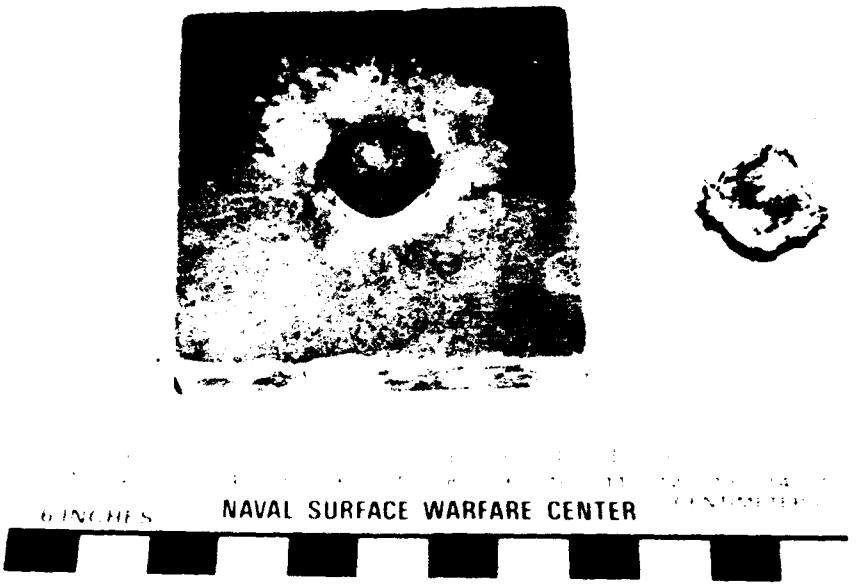

(a) Impact Surface of Steel Plate; Back Surface of Cube

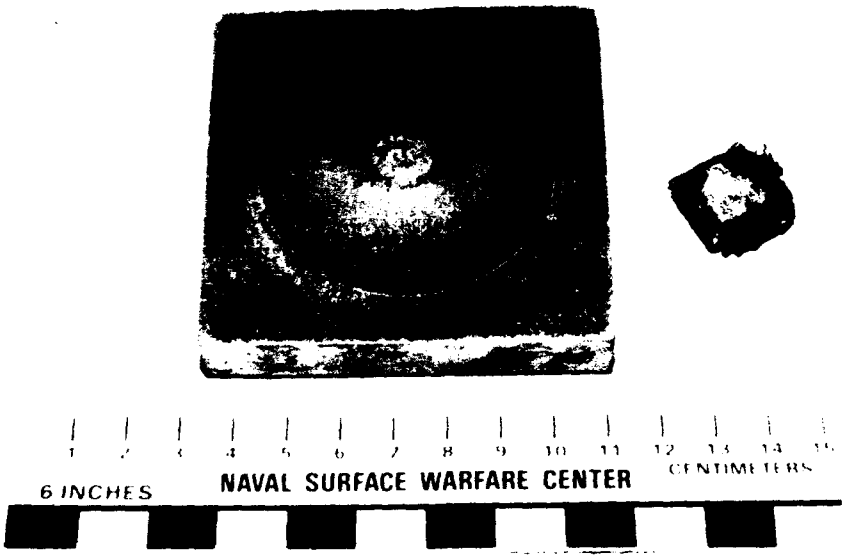

(b) Back Surface of Steel Plate, Impact Surface of Cube

FIGURE A-2. RECOVERED 0.518-IN.-THICK MILD STEEL TARGET PLATE AND CUBE FOR EXPERIMENT 2 (TARGET MASS = 599 GM; IMPACT VELOCITY = 2013 FT/SEC)

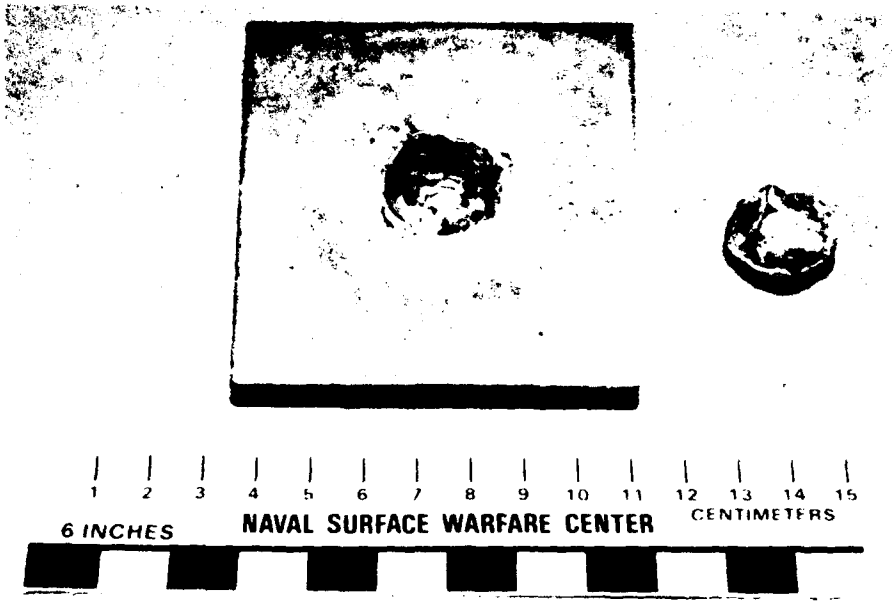

(a) Impact Surface of Steel Plate; Back Surface of Cube

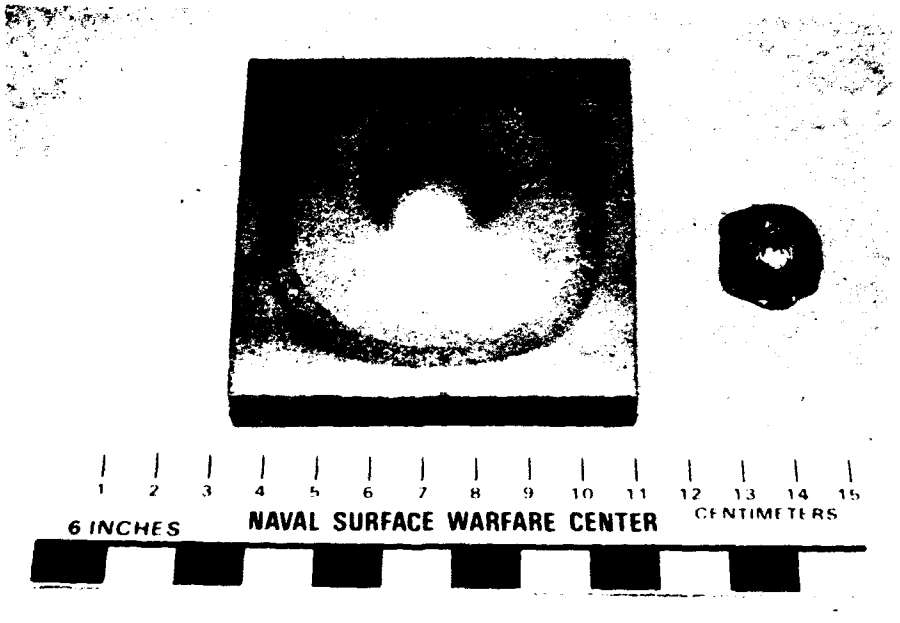

(b) Back Surface of Steel Plate, Impact Surface of Cube

FIGURE A-3. RECOVERED 0.495-IN.-THICK 1018 STEEL TARGET PLATE AND CUBE FOR EXPERIMENT 3 (TARGET MASS = 569 GM; IMPACT VELOCITY = 2516 FT/SEC)

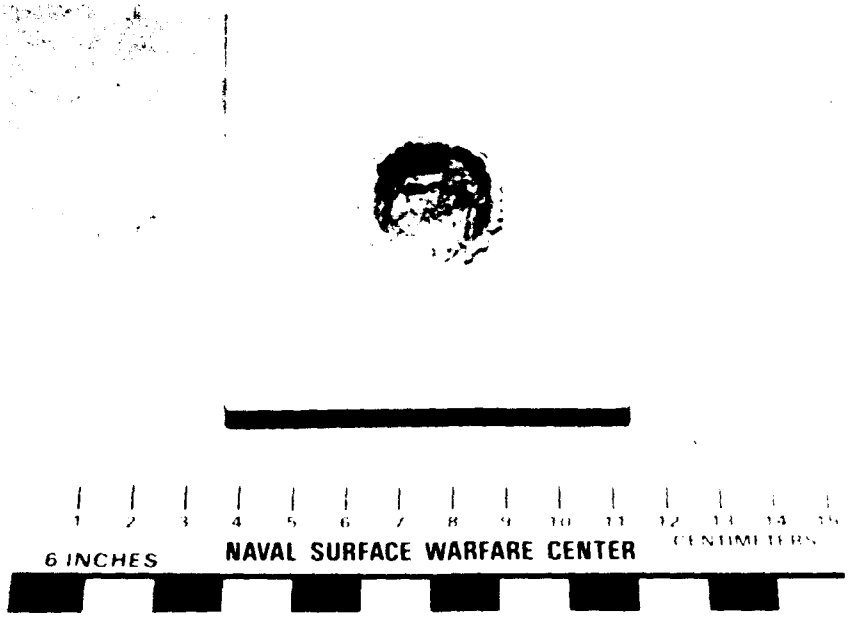

(a) Impact Surface of Steel Plate; Back Surface of Embedded Cube

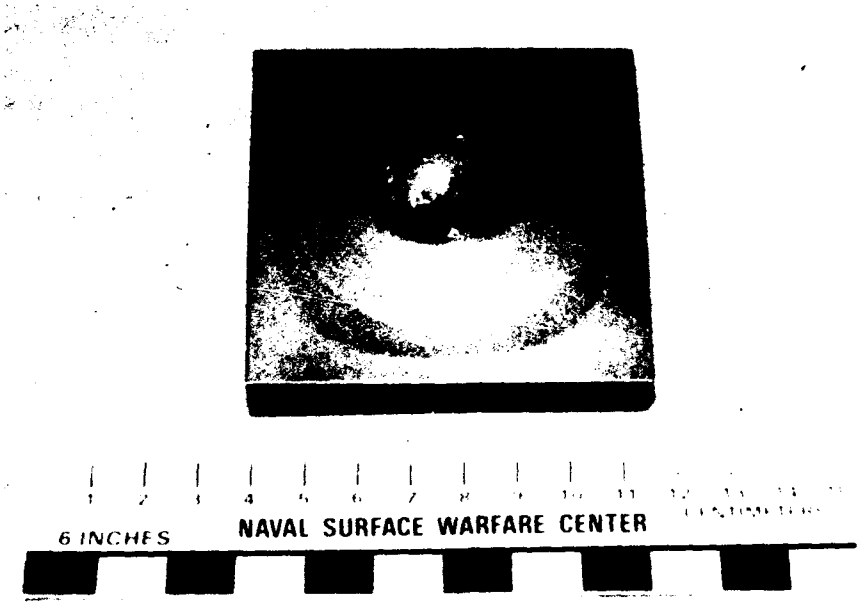

(b) Back Surface of Steel Plate

FIGURE A-4. RECOVERED 0.495-IN.-THICK 1018 STEEL TARGET PLATE WITH EMBEDDED CUBE FOR EXPERIMENT 4 (TARGET MASS = 570 GM; IMPACT VELOCITY = 3106 FT/SEC)

(a) Impact Surface of Steel Plate; Back Surface of Embedded Cube

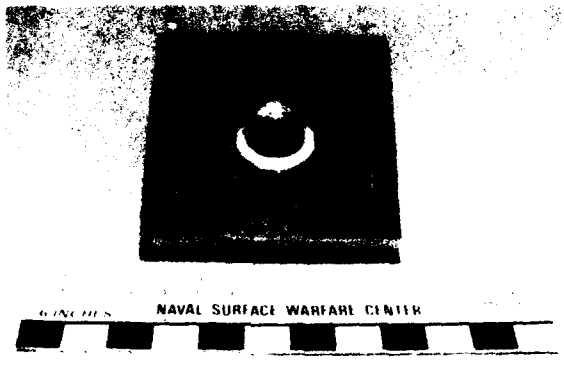

(b) Back Surface of Steel Plate

(c) Side View of Steel Plate

FIGURE A-5. RECOVERED 0.522-IN.-THICK NARROW-RIBBED 1018 STEEL TARGET PLATE WITH EMBEDDED CUBE FOR EXPERIMENT 5 (TARGET MASS = 569 GM; IMPACT VELOCITY = 3101 FT/SEC)

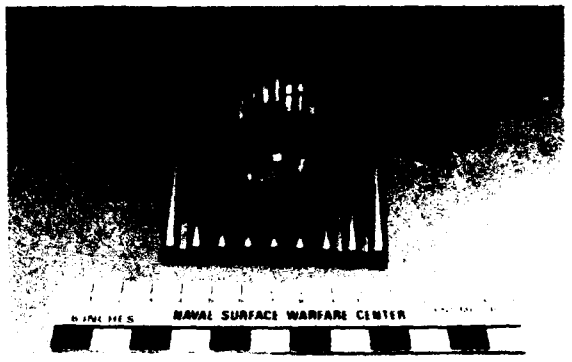

(a) Impact Surface of Steel Plate; Back Surface of Embedded Cube

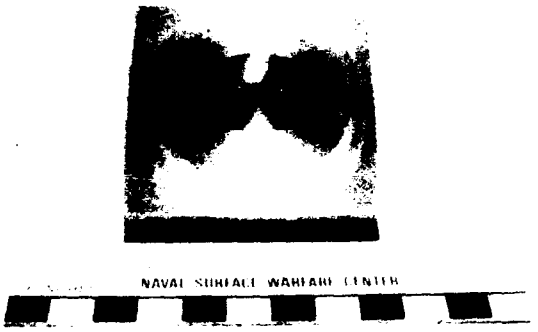

(b) Back Surface of Steel Plate

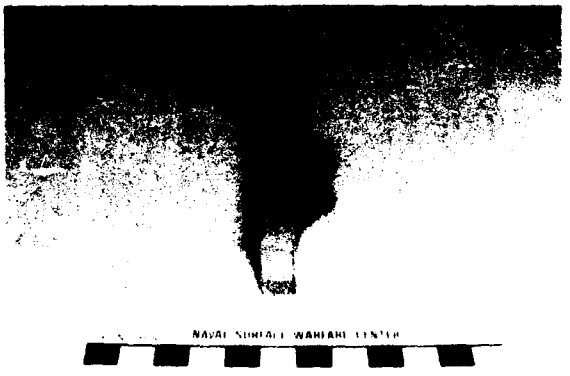

(c) Side View of Steel Plate

FIGURE A-6. RECOVERED 0.545-IN.-THICK WIDE-RIBBED 1018 STEEL TARGET PLATE WITH EMBEDDED CUBE FOR EXPERIMENT 6 (TARGET MASS = 568 GM; IMPACT VELOCITY = 3064 FT/SEC)

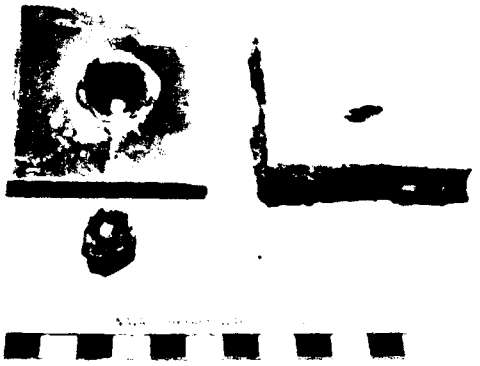

(a) Impact Surface of Steel Plate; Front Surface of Kevlar/Epoxy Layer; Back Surface of Cube

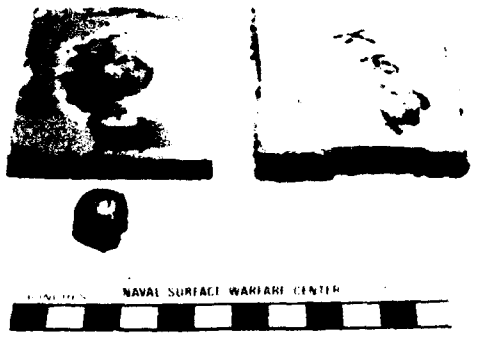

(b) Back Surface of Steel Layer; Back Surface of Kevlar/Epoxy Layer; Impact Surface of Cube

(c) Side View of Steel and Kevlar/Epoxy Layers; Impact Surface of Cube

FIGURE A-7. RECOVERED TWO-LAYER 0.923-IN.-THICK TARGET PLATE AND CUBE FOR EXPERIMENT 7 (LAYER 1: 0.416-IN.-THICK 1018 STEEL; LAYER 2: 0.507-IN.-THICK KEVLAR/EPOXY) (TARGET MASS = 579 GM; IMPACT VELOCITY = 3084 FT/SEC)

(a) Impact Surface of Kevlar/Epoxy Layer with Embedded Cube

(b) Back Surface of Steel Layer

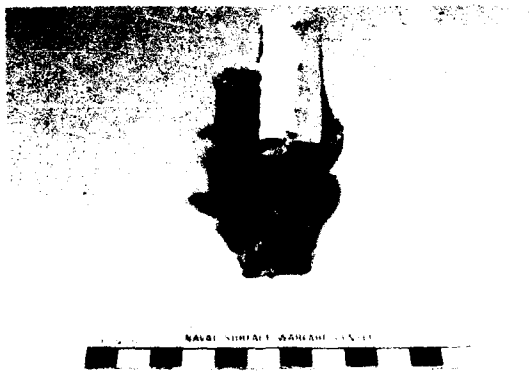

(c) Side View of Kevlar/Epoxy and Steel Layers

FIGURE A-8. RECOVERED TWO-LAYER 0.923-IN.-THICK TARGET PLATE WITH EMBEDDED CUBE FOR EXPERIMENT 8 (LAYER 1: 0.507-IN.-THICK KEVLAR/EPOXY; LAYER 2: 0.417-IN.-THICK 1018 STEEL) (TARGET MASS = 579 GM; IMPACT VELOCITY = 3082 FT/SEC)

(a) Fragmented Cermet Layer;
Front Surface of Steel Layer; Back Surface of Cube

(b) Fragmented Cermet Layer;
Back Surface of Steel Layer; Impact Surface of Cube

(c) Fragmented Cermet Layer;
Side View of Steel Layer; Impact Surface of Cube

FIGURE A-9. RECOVERED TWO-LAYER 0.726-IN.-THICK TARGET PLATE AND CUBE FOR EXPERIMENT 9 (LAYER 1: 0.366-IN.-THICK ALUMINUM OXIDE-BASED CERMET; LAYER 2: 0.360-IN.-THICK 304 STAINLESS STEEL) (TARGET MASS = 587 GM; IMPACT VELOCITY = 3037 FT/SEC)

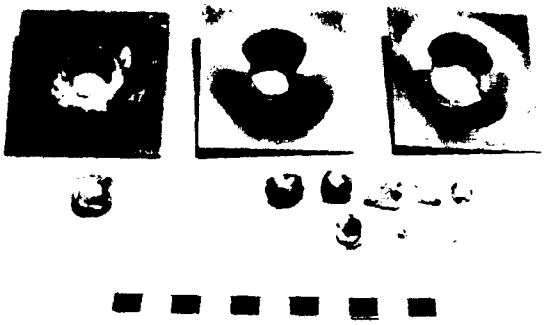

(a) Impact Surface of Layer 1; Front Surfaces of Layers 2 and 3; Some Fragment Pieces; Back Surface of Cube (Shown on Left)

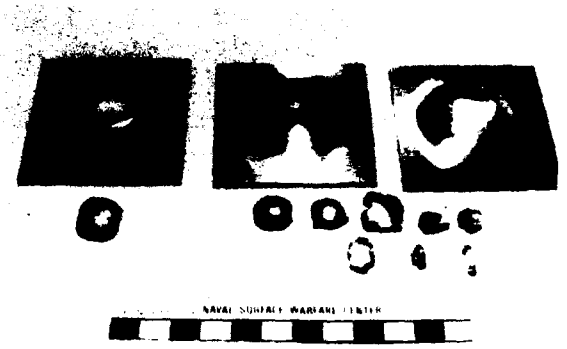

(b) Back Surfaces of Layers 1, 2, and 3; Some Fragment Pieces; Impact Surface of Cube (Shown on Left)

(c) Side View of Three Steel Layers; Some Fragment Pieces: Back Surface of Cube (Shown on Left)

FIGURE A-10. RECOVERED THREE-LAYER 0.500-IN.-THICK TARGET PLATE AND CUBE FOR EXPERIMENT 10 (LAYER 1: 0.167-IN.-THICK 1018 STEEL; LAYER 2: 0.166-IN.- THICK 1018 STEEL; LAYER 3: 0.167-IN.-THICK 1018 STEEL) (TARGET MASS = 576 GM; IMPACT VELOCITY = 3091 FT/SEC)

(a) Impact Surface of Layered Target; Some Fragment Pieces; Back Surface of Cube (Shown on Right)

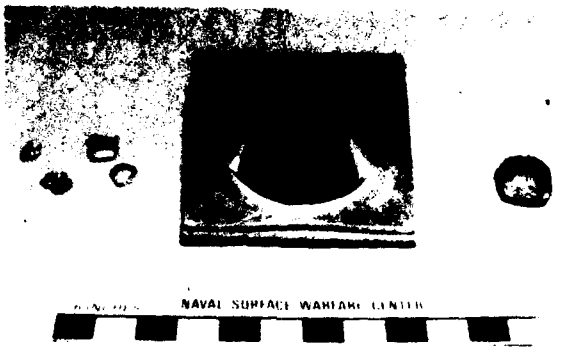

(b) Back Surfaces of Layered Target; Some Fragment Pieces; Impact Surface of Cube (Shown on Right)

(c) Side View of Layered Target; Some Fragment Pieces; Impact Surface of Cube (Shown on Left)

FIGURE A-11. RECOVERED THREE-LAYER 0.501-IN.-THICK TARGET PLATE AND CUBE FOR EXPERIMENT 11 (LAYER 1: 0.168-IN.-THICK MILD STEEL; LAYER 2: 0.172-IN.- THICK 6061-0 ALUMINUM; LAYER 3: 0.161-IN.-THICK MILD STEEL) (TARGET MASS = 422 GM; IMPACT VELOCITY = 3079 FT/SEC)

(a) Fragmented Pieces from Ceramic Tile Layers; Front Surfaces of Steel Layer and Steel Fragments; Back Surface of Cube (Shown on Left)

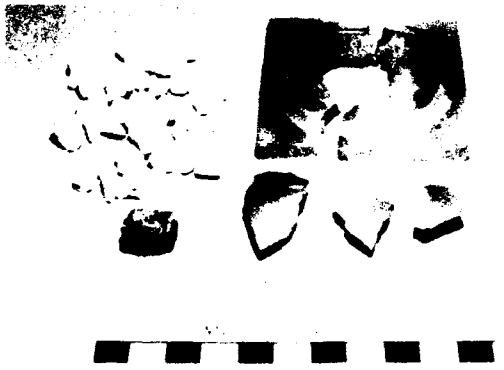

(b) Fragmented Pieces from Ceramic Tile Layers; Back Surfaces of Steel Layer and Steel Fragments; Impact Surface of Cube (Shown on Left)

(c) Fragmented Pieces from Ceramic Tile Layers; Side View of Steel Layer; Back Surface of Steel Fragments; Impact Surface of Cube (Shown on Right)

FIGURE A-12. RECOVERED FOUR-LAYER 0.919-IN.-THICK TARGET PLATE AND CUBE FOR EXPERIMENT 12 (LAYER 1: 0.250-IN.-THICK CERAMIC TILE; LAYER 2: 0.039-IN.- THICK TORR-SEAL EPOXY; LAYER 3: 0.250-IN.-THICK CERAMIC TILE; LAYER 4: 0.380-IN.-THICK 1018 STEEL) (TARGET MASS = 634 GM; IMPACT VELOCITY = 3070 FT/SEC)

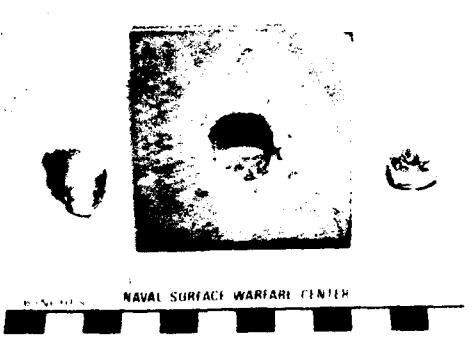

(a) Impact Surface of Layered Target; a Fragment Piece; Back Surface of Cube (Shown on Right)

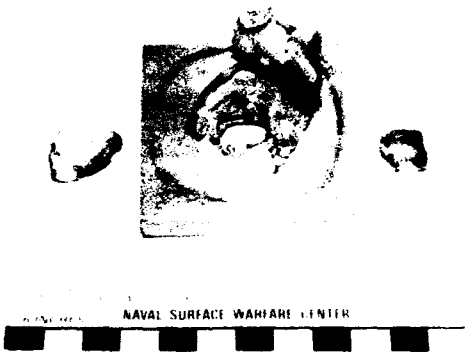

(b) Back Surface of Layered Target; a Fragment Piece; Impact Surface of Cube (Shown on Right)

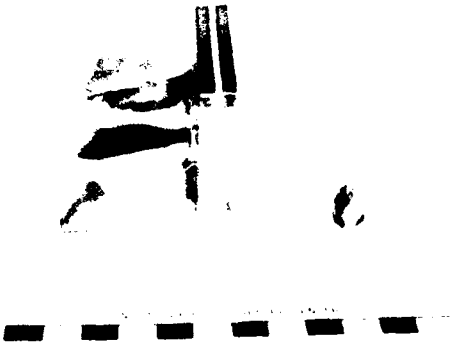

(c) Side View of Layered Target; a Fragment Piece; Side View of Cube (Shown on Right)

FIGURE A-13. RECOVERED FIVE-LAYER 0.499-IN.-THICK TARGET PLATE AND CUBE FOR EXPERIMENT 13 (LAYER 1: 0.175-IN.-THICK MILD STEEL; LAYER 2: 0.045-IN.- THICK GRADE A TITANIUM; LAYER 3: 0.086-IN.-THICK 6061-0 ALUMINUM; LAYER 4: 0.050-IN.-THICK GRADE A TITANIUM; LAYER 5: 0.143-IN.-THICK MILD STEEL) (TARGET MASS = 423 GM; IMPACT VELOCITY = 3112 FT/SEC)

(a) Impact Surface of Layered Target; a Fragment Piece; Back Surface of Cube (Shown on Right)

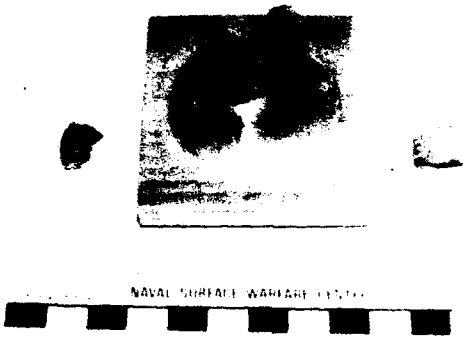

(b) Back Surface of Layered Target; a Fragment Piece; Impact Surface of Cube (Shown on Right)

(c) Side View of Layered Target; a Fragment Piece; Side View of Cube (Shown on Right)

FIGURE A-14. RECOVERED FIVE-LAYER 0.503-IN.-THICK TARGET PLATE AND CUBE FOR EXPERIMENT 14 (LAYER 1: 0.153-IN.-THICK HADFIELD STEEL; LAYER 2: 0.051-IN.- THICK GRADE A TITANIUM; LAYER 3: 0.087-IN.-THICK 6061-0 ALUMINUM; LAYER 4: 0.051-IN.-THICK GRADE A TITANIUM; LAYER 5: 0.161-IN.-THICK HADFIELD STEEL) (TARGET MASS = 474 GM; IMPACT VELOCITY = 3114 FT/SEC)

DISTRIBUTION

	Copies
DOD ACTIVITIES (CONUS)	
ATTN OP-987B	1
COMMANDER	
OFFICE OF CHIEF OF NAVAL OPS	
NAVY DEPARTMENT	
WASHINGTON DC 20350-2000	
ATTN SEA 91WM	1
SEA 06AR	1
PMS 413	1
PMQ 4221 GARRISON	1
COMMANDER	
NAVAL SEA SYSTEMS COMMAND	
WASHINGTON DC 20362-5101	
ATTN A C HOLT	1
G KOPCSAK	1
T HITCHCOCK	1
COMMANDER	
OFFICE OF MUNITIONS	
OFFICE OF UNDERSECRETARY OF DEFENSE	
WASHINGTON DC 20301	
ATTN OCNR213 SIEGEL	1
CHIEF OF NAVAL RESEARCH	
OFFICE OF NAVAL RESEARCH	
TECHNOLOGY DIRECTORATE	
800 N QUINCY AVE	
ARLINGTON VA 22217-5660	
ATTN C DETTLING (CODE C27B1)	1
S A FINNEGAN	1
N FASIG	1
J WEEKS	1
COMMANDER	
NAVAL AIR WARFARE CENTER	
CHINA LAKE CA 93555-6001	
ATTN R GARISON CODE 17403	1
COMMANDER	
NAVAL SURFACE WARFARE CENTER	
CARDEROCK DIVISION	
BETHESDA MD 20084-5000	

	Copies
DOD ACTIVITIES (CONUS) (Cont.)	
ATTN STEVE FISHMAN	1
JUDAH GOLDWASSER (Code 332PE)	1
RICHARD MILLER	1
DICK WILLIAMS	1
COMMANDER	
OFFICE OF NAVAL RESEARCH	
800 N QUINCY AVE	
ARLINGTON VA 22217-5660	
ATTN E J RINEHART	1
COMMANDER	
FIELD COMMAND	
DEFENSE NUCLEAR AGENCY	
FCDNA/FCTP	
KIRTLAND AFB NM 87117	
ATTN J GRIFFITH	1
J R McDONALD (CODE 6110)	
A WILLIAMS	1
COMMANDER	
NAVAL RESEARCH LABORATORY	
WASHINGTON DC 20350	
ATTN F GRACE	1
G E HAUVER	1
A DIETRICH	1
J KINEKE	1
R COATS	1
J DEHN	1
DIRECTOR	
ARMY RESEARCH LABORATORY	
ABERDEEN PROVING GROUND MD 21005	
ATTN W MARLEY ST3	1
DIRECTOR	
ARMY FOREIGN SCIENCE AND TECHNOLOGY CENTER	
220 SEVENTH ST N E	
CHARLOTTESVILLE VA 22901-5396	

DISTRIBUTION (Continued)

	Copies
DOD ACTIVITIES (CONUS) (Cont.)	
ATTN JIM BILLINGSLEY	1
DON LOVELACE	1
DIRECTOR	
ARMY MISSILE COMMAND	
RD&E CENTER	
AMSMI-RD-SS-AA	
REDSTONE ARSENAL AL 35898	
ATTN R W KOCHER LSO	1
DEFENSE ADVANCED RESEARCH PROJECTS AGENCY	
3701 N FAIRFAX DR	
ARLINGTON VA 22203-1714	
ATTN K PETERSEN	1
K BRADLEY	1
DEFENSE NUCLEAR AGENCY	
6801 TELEGRAPH RD	
ALEXANDRIA VA 22310-3398	
NON-DOD ACTIVITIES	
ATTN W DANEN	1
L HULL	1
J M HOLT	1
J W HOPSON	1
J REPA	1
S SHEFFIELD	1
S R SKAGGS	1
TECHNICAL LIBRARY	1
LOS ALAMOS NATIONAL LABORATORY	
LOS ALAMOS NM 87544	
ATTN W J NELLIS	1
LAWRENCE LIVERMORE NATIONAL LABORATORY	
P O BOX 808	
LIVERMORE CA 94550	
ATTN C E ANDERSON JR	1
ROBERT YOUNG	1
SOUTHWEST RESEARCH INSTITUTE	
P O DRAWER 28510	
SAN ANTONIO TX 78228	

	Copies
NON-DOD ACTIVITIES (Cont.)	
DEFENSE TECHNICAL INFORMATION CENTER	12
CAMERON STATION	
ALEXANDRIA VA 22304-6145	
ATTN L C CHHABILDAS 1433	1
M J FORRESTAL 9723	1
D E GRADY 1433	1
R A GRAHAM 1153	1
M KIPP 1432	1
V LUK 9723	1
J L WISE 1433	1
TECHNICAL LIBRARY	1
SANDIA NATIONAL LABORATORIES	
ALBUQUERQUE NM 87185	
ATTN D SHOCKEY	1
L SEAMAN	1
T H ANTOUN	1
SRI INTERNATIONAL	
333 RAVENSWOOD AVE	
MENLO PARK CA 94025	
ATTN GIFT AND EXCHANGE DIVISION	4
LIBRARY OF CONGRESS	
WASHINGTON DC 20540	
ATTN R W ARMSTRONG	1
DEPARTMENT OF MECHANICAL ENGINEERING	
UNIVERSITY OF MARYLAND	
COLLEGE PARK MD 20742	
ATTN S J BLESS	1
INSTITUTE FOR ADVANCED TECHNOLOGY	
UNIVERSITY OF TEXAS AT AUSTIN	
4030-2 WEST BRAKER LANE	
AUSTIN TX 78759-5320	
ATTN E L FOSTER	1
F HALL	1
BATTELLE	
505 KING AVENUE	
COLUMBUS OH 43201-2693	

DISTRIBUTION (Continued)

		Copies
INTERNAL		
B05	MOORE	1
B05	STATON	1
E231		3
E232		2
E282	GRAY	1
F107	ADAMS	1
G07	MOORE	1
G20		1
G22		1
G22	DIBBLE	1
G22	GARNETT	1
G22	GRIGSBY	1
G22	HOLT	1
G22	MOCK	1
G22	POSTON	1
G22	SMITH	1
G22	SWIERK	1
G22	VITTORIA	1
G22	WAGGENER	1
G22	WICKS	1
G24	DICKINSON	1
G24	HOCK	1
G24	WASMUND	1
G30		1
G32	HARKINS	1
G32	MCCONKIE	1
G34	FOSTER	1
G205		1
G301	WILSON	1
GH3	YAGLA	1
K22	O'HARA	1
N74	GIDEP	11
R04		1
R11	GOTZMER	1
R13		1
R13	BARDO	1
R13	COFFEY	1
R13	FORBES	1
R13	WILSON	1
R13	ZERILLI	1
R16	ROZNER	1
R31	CLARK	1
R31	HARTMANN	1

		Copies
INTERNAL (Cont.)		
R32	GARRETT	1
R44	SZYMCZAK	1
R101	ROSLUND	1
R101A	REED	1
R10A2		1
R92	MCKEOWN	1

REPORT DOCUMENTATION PAGE

Form Approved
OMB No 0704 0188

1. AGENCY USE ONLY (Leave blank)	2. REPORT DATE	3. REPORT TYPE AND DATES COVERED
	July 1994	Final/June 1994

4. TITLE AND SUBTITLE
Penetration of Solid and Layered Targets by Gas Gun-Launched Steel Cubes

5. FUNDING NUMBERS
IMAD Task 3002B

6. AUTHOR(S)
Willis Mock, Jr. William H. Holt

7. PERFORMING ORGANIZATION NAME(S) AND ADDRESS(ES)
Naval Surface Warfare Center
Dahlgren Division (Code G22)
17320 Dahlgren Road
Dahlgren, VA 22448-5100

8. PERFORMING ORGANIZATION REPORT NUMBER
NSWCDD/TR-93/429

9. SPONSORING/MONITORING AGENCY NAME(S) AND
IMAD Program Office (SEA-91WM1)
Washington, DC 20362

10. SPONSORING/MONITORING AGENCY REPORT NUMBER

11. SUPPLEMENTARY NOTES

12a. DISTRIBUTION/AVAILABILITY
Approved for public release; distribution is unlimited.

12b. DISTRIBUTION CODE

13. ABSTRACT *(Maximum 200 words)*

A series of 14 impact experiments has been performed in which solid and layered targets nominally 3 x 3-in. by 0.5-in. thick have been impacted by 0.5-in. steel cubes in a flat-faced orientation. The number of target layers varied from one to five. The areal density of the targets ranged from 3.6 to 11.1 gm/cm^2. Three experiments were performed at an impact velocity ranging from 2000 to 2500 ft/sec and eleven experiments were performed at a velocity of approximately 3100 ft/sec. Target perforation did not occur in six of the higher velocity experiments. For these experiments, the number of target layers was either one or two. Target perforation occurred in five of the higher velocity experiments; the number of target layers was either three, four, or five for these experiments. Target failure consisted of one or more of the following types: cratering, shear bands, shear plugging, fracture, plate bending, petalling, and fiber breaking.

The impact resistance of a single flat-faced 1018 steel target was not significantly improved by machining a series of parallel ribs on the impact face of a target plate with the same areal density. These targets failed by a combination of shear banding and bending fracture. The results for the two-layer target of 1018 steel and Kevlar/epoxy composite showed that less steel fracture occurred when the composite was placed on the back surface of the impacted steel layer rather than on front of it. For the two-layer aluminum oxide-based cermet-304 stainless steel target, the brittle cermet layer fragmented on cube impact, but only plate bulging and bending occurred in the back surface steel layer.

Target perforation occurred in all of the three-, four-, and five-layer targets. The three-layer 1018 steel target had less impact resistance than the steel single-layer target with the same total thickness. In general, for the metal layered targets, the impacted layer failed by shear plugging and the back surface layer failed by plate bending, petalling, and fracture. Some permanent separation of the metal plates occurred for all the metal-layered-target experiments.

14. SUBJECT TERMS	15. NUMBER OF PAGES
gas gun, oriented launched cube impact, high velocity, penetration, metal target, layered target, fracture, shear bands, plate bending, target failure	41
	16. PRICE CODE

17. SECURITY CLASSIFICATION OF REPORT	18. SECURITY CLASSIFICATION OF THIS PAGE	19. SECURITY CLASSIFICATION OF ABSTRACT	20. LIMITATION OF ABSTRACT
UNCLASSIFIED	UNCLASSIFIED	UNCLASSIFIED	SAR

GENERAL INSTRUCTIONS FOR COMPLETING SF 298

The Report Documentation Page (RDP) is used in announcing and cataloging reports. It is important that this information be consistent with the rest of the report, particularly the cover and its title page. Instructions for filling in each block of the form follow. It is important to ***stay within the lines*** to meet ***optical scanning requirements***.

Block 1. Agency Use Only *(Leave blank)*.

Block 2. Report Date. Full publication date including day, month, and year, if available (e.g. 1 Jan 88). Must cite at least the year.

Block 3. Type of Report and Dates Covered. State whether report is interim, final, etc. If applicable, enter inclusive report dates (e.g. 10 Jun 87 - 30 Jun 88).

Block 4. Title and Subtitle. A title is taken from the part of the report that provides the most meaningful and complete information. When a report is prepared in more than one volume, repeat the primary title, add volume number, and include subtitle for the specific volume. On classified documents enter the title classification in parentheses.

Block 5. Funding Numbers. To include contract and grant numbers; may include program element number(s), project number(s), task number(s), and work unit number(s). Use the following labels:

C	- Contract	PR	- Project
G	- Grant	TA	- Task
PE	- Program Element	WU	- Work Unit Accession No.

BLOCK 6. Author(s). Name(s) of person(s) responsible for writing the report, performing the research, or credited with the content of the report. If editor or compiler, this should follow the name(s).

Block 7. Performing Organization Name(s) and address(es). Self-explanatory.

Block 8. Performing Organization Report Number. Enter the unique alphanumeric report number(s) assigned by the organization performing the report.

Block 9. Sponsoring/Monitoring Agency Name(s) and Address(es). Self-explanatory.

Block 10. Sponsoring/Monitoring Agency Report Number. *(If Known)*

Block 11. Supplementary Notes. Enter information not included elsewhere such as: Prepared in cooperation with...; Trans. of...; To be published in.... When a report is revised, include a statement whether the new report supersedes or supplements the older report.

Block 12a. Distribution/Availability Statement. Denotes public availability or limitations. Cite any availability to the public. Enter additional limitations or special markings in all capitals (e.g. NOFORN, REL, ITAR).

DOD	- See DoDD 5230.24, "Distribution Statements on Technical Documents."
DOE	- See authorities.
NASA	- See Handbook NHB 2200.2
NTIS	- Leave blank

Block 12b. Distribution Code.

DOD	- Leave blank.
DOE	- Enter DOE distribution categories from the Standard Distribution for Unclassified Scientific and Technical Reports.
NASA	- Leave blank.
NTIS	- Leave blank.

Block 13. Abstract. Include a brief ***(Maximum 200 words)*** factual summary of the most significant information contained in the report.

Block 14. Subject Terms. Keywords or phrases identifying major subjects in the report.

Block 15. Number of Pages. Enter the total number of pages.

Block 16. Price Code. Enter appropriate price code ***(NTIS only)***

Block 17.-19. Security Classifications. Self-explanatory. Enter U.S. Security Classification in accordance with U.S. Security Regulations (i.e., UNCLASSIFIED). If form contains classified information, stamp classification on the top and bottom of this page.

Block 20. Limitation of Abstract. This block must be completed to assign a limitation to the abstract. Enter either UL (unlimited or SAR (same as report). An entry in this block is necessary if the abstract is to be limited. If blank, the abstract is assumed to be unlimited.